SONOPHORETIC DELIVERY OF A MODEL MACROMOLECULAR DRUG

A thesis presented in fulfilment of the requirements for the degree of

Master of Philosophy

by

SUMEIA M. MOHAMED

STRATHCLYDE INSTITUTE OF PHARMACY AND BIOMEDICAL SCIENCES

UNIVERSITY OF STRATHCLYDE

27 TAYLOR STREET

GLASGOW G4 0NR

DEDICATION

This thesis is dedicated to

My father, Mohamed

My husband, Ahmed

For all the wonderful things they do for me and for supporting me all the way.

ACKNOWLEDGEMENTS

All thanks to my God who helped me to complete this work and I would like to acknowledge and extend my heartfelt gratitude to:

Dr Victor Meidan for his support and encouragement, which has made the completion of this project possible.

Prof Gillian Eccleston, for her advice during the work of this project.

Dr Dino Rotondo and Dr Jillian Davidson, for their help in teaching me the various steps of the ELISA technique.

Dr Anthony Gachagan at the Strathclyde Centre for Ultrasonic Engineering for helping with the acoustic calibration methods.

ABSTRACT

The use of low frequency ultrasound as a physical enhancer for transdermal drug delivery is known as sonophoresis. This science is still in its infancy. The aim of this study was to explore how low frequency ultrasound can be used to enhance the transdermal delivery of a model macromolecular drug. Initial studies aimed to validate the output of the ultrasound generator. Hydrophone measurements showed that the actual frequency was very close to the supplier's stated 20kHz value while calorimetric measurements showed that the actual intensities were close to and proportional to that stated by the generator's amplitude dial. Interferon-gamma, with a molecular weight of 17000 Da, was chosen as a model macromolecular drug while transport studies were carried out using full-thickness porcine skins inserted in Franz cells. An ultrasound beam (10% duty cycle) of SATA intensity 3.7 W/cm^2 was applied for periods not exceeding 5 minutes thus keeping skin surface temperatures from exceeding control levels by more than 3ºC. Whereas passive macromolecule flux was virtually zero, 5 minutes sonication allowed about 50 ng $/cm^2$ drug to permeate transdermally. Drug transport could be significantly improved by pretreating the skin with sodium lauryl sulphate solution prior to the sonication step. This allowed permeation to reach over 100 ng $/cm^2$. However, all other tested chemical enhancers – sodum octyl sulphate, sodium eicosyl sulphate, menthone, carvone, alpha terpineol, oleic acid, linoleic acid and stearic acid did not show such an additive interaction with ultrasound. Interestingly, most of the cumulative permeation profiles were not of the typical lag time followed by linear steady state type. The peculiar effectivity of sodium lauryl sulphate and the irregular permeation profiles require further investigation in order to determine the mechanisms occurring.

LIST OF CONTENTS

CHAPTER 3: INTERFERON-GAMMA TRANSPORT STUDIES

CHAPTER 1: INTRODUCTION

1.1 ORGANISATION OF THIS CHAPTER

Sonophoresis is defined as the use of low frequency ultrasound to permeabilise the skin to drug molecules. The subject of this current project is to use this approach to transdermally deliver a model macromolecule. This first chapter starts by describing the anatomical structure of human skin and its different layers. This is followed by a description of the principles of passive transdermal drug absorption including its physicochemical basis, the penetration pathways used by drugs and the factors influencing the process. The next section describes sonophoresis and includes a literature review of this technology. Important aspects such as the background, skin changes, mechanisms and clinical aspects are separately considered. The final section of this Introduction explains the particular aims and objectives of the present project.

1.2 THE STRUCTURE OF HUMAN SKIN

The skin is by far the largest organ in the human body, covering a surface area of approximately $2m^2$ and receiving about one third of the body's entire blood circulation. The main role of human skin is to exert a protective function in terms of preventing external microbes and chemicals penetrating the body. It also plays a role in temperature control and provides protection for the body against mechanical shocks and injury. However, the very large surface area of the skin means it is potentially attractive for use in drug delivery applications.

The transdermal delivery approach has many advantages over the more conventional oral treatment. These include the avoidance of first-pass metabolism; treatment can be quickly started or stopped; the rate of systemic delivery can be more uniformly maintained and better patient compliance is achieved. Obviously, the transdermal route also provides the clinician with a possible extra therapeutic option for patient therapy. Disadvantages include the potential for localized irritation or allergies and difficulties associated with the time necessary for a drug to diffuse through skin (Bomer et al, 1994).

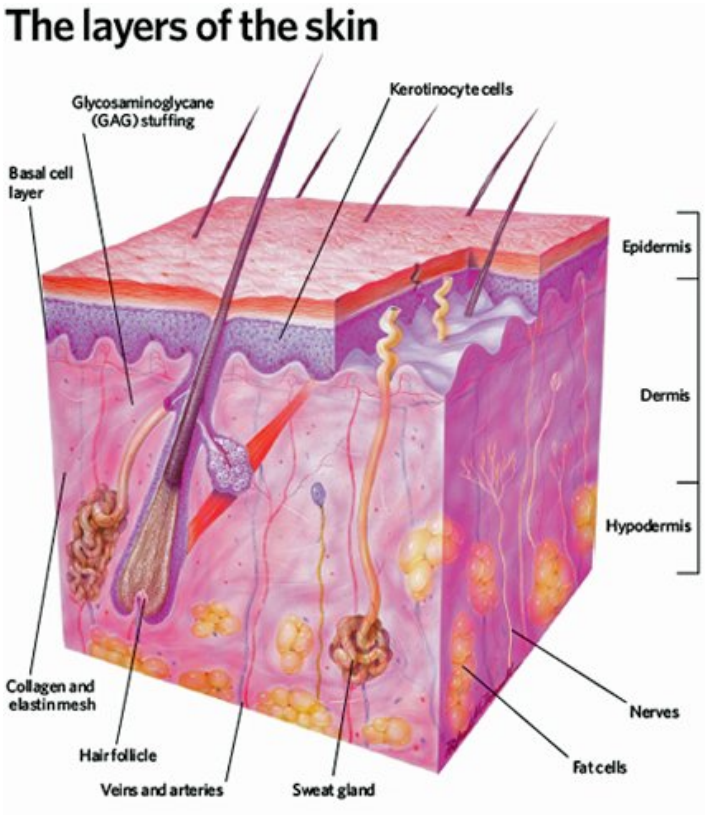

Fig. 1.1: Diagram showing the different layers of human skin. From: http://www.cosmosmagazine.com/files/mar08/20080318_skin_structure.jpg

In order to understand the principles of percutaneous drug delivery, it is important to firstly understand skin structure. The skin is composed of several layers including the epidermis, dermis and underlying subcutaneous tissues. The subcutaneous tissues are also known as the hypodermis. Figure 1.1 shows a cross-sectional representation of human skin. The next sections each deal with different skin layers.

1.2.1 The Epidermis

This is a tissue that receives nutrients from the underlying capillaries. The nutrients diffuse in across the basement membrane which separates the epidermis from the

underlying dermis. Within the epidermis there are embedded various appendages such as hair follicles, sebaceous glands, eccrine sweat glands and in some places apocrine sweat glands. All these are supported by a rich vascular network. The epidermis actually consists of two layers. The viable epidermis is the lower layer and this has a typical thickness of 50 to 100 μm. The density of this layer is similar to that of water. The viable epidermis is actually in a state of continuous change as it is composed of many layers of keratinocytes at different stages of differentiation. At the bottom, there are actively dividing keratinocytes that are gradually migrating upwards. These cells mature, change and actually begin to die as they slowly move upward. In particular, the keratinocytes slowly transform into unviable, flattened and keratin-loaded cells known as corneocytes. It takes about 2 weeks for the cells to move from the bottom of the viable epidermis to its top. The spaces between the keratinocytes and corneocytes contain corneodesmosomes. These contribute to the mechanical strength of the viable epidermis.

The upper layer of epidermis is the stratum corneum or horny layer. This consists of the corneocytes formed in the underlying viable epidermis that are mostly mixed in lamellar crystalline lipids. The stratum corneum usually consists of some 10 to 20 such cells stacked up upon each other. The gaps between the corneocytes are filled with various lipids such as cholesterol, ceramides and long chain free fatty acids. Other constituents of the stratum corneum include phospholipids, glycosphingolipids and other neutral lipids as well as some proteins like keratin. At the top, the corneocytes are lost from the skin surface in a process termed desquamation and this removal provides space for new corneocytes to migrate upwards from the viable

epidermis. It takes 2 weeks for the corneocytes at the base of the stratum corneum to be sloughed off from the skin (Schaefer and Redelmeier, 1996). The stratum corneum may be about 15 to 20 μm in thickness but it can be a lot thicker at certain sites of the body such as the sole of the foot. The skin is also thinner when dry but can swell up to several times its thickness upon hydration. This is due to the potential for very large amounts of water uptake (Verdier-Sevrain and Bonte, 2007). The stratum corneum is actually the main barrier to most inwardly diffusing substances applied on to the skin surface. It is also allows effective activity of the immune system.

1.2.2 The Dermis

The basal cell layer with its associated basement membrane represents the boundary between the viable epidermis and the underlying dermis. As Fig. 1 shows, the basal cell layer is tortuous and dermal papillae extend into the epidermis. The dermis itself is usually about 2-3mm thick and it makes the largest contribution to the mass of the skin (Barry, 1983). The tissue consists of a non-cellular scaffold of fibrous connective tissue implanted in an amorphous mucopolysaccharide gel-like material (Uitto et al., 1993). The collagenous fibres in the dermis account for 70% of the dry weight of the skin. There are also elastic fibres present and these form the second most important component by weight. This set of fibres, which is often associated with hair follicles, provides the elasticity necessary for dermal shape retention. Other constituents such as chondroitin sulphate, heparin and heparin sulphate can bind huge amounts of water and this provides moisture-retentive properties to the tissue (Schaefer and Redelmeier, 1996). In addition, the dermis contains an

extensive network of capillaries, lymphatic vessels and nerves and it acts as a mechanical support for all these. The blood vessels which reside within the dermis reach to within 200 μm of the skin surface (Barry, 1983). In terms of drug delivery, this ensures that compounds which permeate across the skin are rapidly swept away by the systemic blood supply, thus ensuring that drug concentration in the dermis remains tiny.

1.2.3 Subcutaneous Connective Tissues

The subcutaneous tissue or hypodermis is not always considered a true part of the structure of the skin. It is composed of loose textured, white, fibrous connective tissue intermingled with both elastic fibres and fat cells known as adipocytes. The main role of this layer is to provide protection to the body against mechanical trauma, provide thermal insulation and contain a store of fats as an energy source. The hypodermis also contains; blood vessels, lymph vessels, the base of hair follicles, secretory portions of the sweat glands as well as cutaneous nerves. Most investigators believe that drugs permeating the skin will in most cases enter the circulatory system long before reaching the hypodermis. Although it should be noted that fat tissue can serve as a depot or reservoir for certain drugs.

1.3 THE PRINCIPLES OF TRANSDERMAL DRUG ABSORPTION

1.3.1 Fundamentals of Drug Diffusion

Passive diffusion is essentially the transfer of molecules from an area of where they exist at high concentration to that of where they exist at low concentration. This movement is a consequence of the random Brownian motion of molecules. For transdermal delivery, the slowest and rate limiting step for the diffusion of most compounds occurs in the stratum corneum. However, the viable epidermis or dermis may exert a rate limiting effect in situations when the applied compound is very lipophilic (Frum et al., 2007). The mathematics of passive drug diffusion are described by Fick's first law of diffusion. It states that the per unit area transfer rate of a solute across a test membrane is proportional to the solute concentration gradient. This can presented as the equation:

$$J = -D\frac{\partial C}{\partial x} \tag{1.1}$$

Where J is the rate of transfer per unit area of surface, C is the concentration of solute, x is the test membrane thickness and D is the solute diffusion coefficient. The negative sign signifies that solute flux is in the direction of reducing concentration. The units of diffusivity are $cm^2\ s^{-1}$.

During transdermal drug delivery investigations, a two compartment-model is often used with sink conditions. This is shown as:

$$J = \frac{DK\,(C_{app.} - C_{rec.})}{h} \tag{1.2}$$

Where K is the partition coefficient of the solute, h is membrane thickness, $C_{app} - C_{rec}$ is the concentration gradient in which C_{app} is the applied solute concentration in the donor compartment and C_{rec} is solute concentration in the receiver compartment. During sink conditions, Equation 1.2 can be condensed into:

$$J = k_p . C_{app.} \tag{1.3}$$

Where k_p (=KD/h) is the permeability coefficient.

Fig. 1.2 shows a typical plot of cumulative drug amount as a function of time for a drug permeating through skin into the systemic circulation. If the linear, steady-state segment of the curve is back-extrapolated to where it meets the time axis, the intercept obtained is the lag time, L, which is given by:

$$L = \frac{h^2}{6D} \tag{1.4}$$

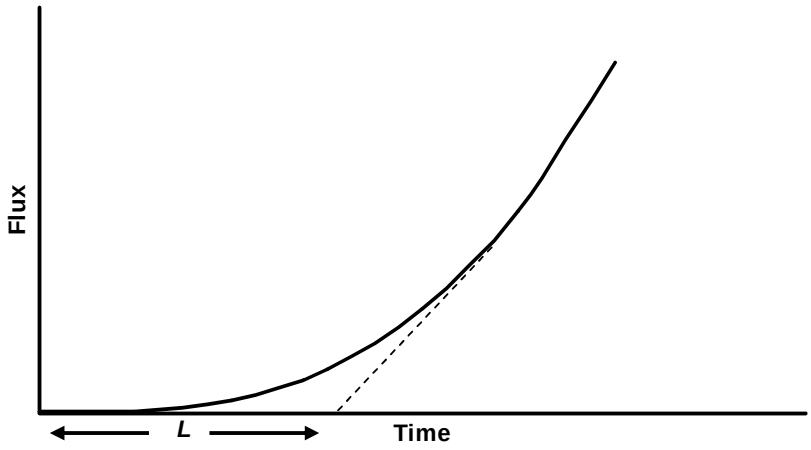

Fig.1.2: Steady state is achieved when the plot becomes linear; extrapolation of the linear portion to the time axis yields the lag time L.

1.3.2 Drug Absorption Pathways in the Stratum Corneum

Once a drug has partitioned into the stratum corneum, it diffuses through this layer as a result of the concentration gradient mentioned above. This transfer of drug may occur along two alternative permeation pathways - an intercellular and a transcellular pathway (Doukas and Kollias, 2004). The intercellular pathway involves drug diffusion through the lipid bilayers existing between the keratinocytes. This means the drug would follow a very tortuous route that would mean the diffusion distance would actually be much longer than the thickness of the stratum corneum. The transcellular pathway involves drug diffusion directly through the keratinocytes but this would still involve some diffusion through lipid bilayers existing between keratinocytes. The relative importance of the intercellular or the transcellular pathways is still controversial. Hydrophilic drugs may mostly select the transcellular pathway while lipophilic drugs might mostly use the intercellular pathway. Yet there is growing evidence that the intercellular pathway could predominate in most cases (Schaefer and Redelmeier, 1996).

A third and still questionable potential pathway is the transappendageal or transfollicular route. This involves compounds permeating down through the hair follicles and perhaps the associated sebaceous glands (Meidan et al., 2005). It was historically assumed that these structures only played a significant role during the initial, non-steady state phase of absorption. However, recent studies using various new stripping techniques suggest that the hair follicles may be more important for drug absorption than once assumed (Knorr et al., 2009). In particular, the follicular pathway might be significant in the case of highly hydrophilic or large molecules

(Mitragotri et al., 2003). The overall significance and contribution of the hair follicles is still debatable at this time (Meidan et al., 2005). Fig. 1.3 shows all three routes schematically.

Fig. 1.3: Schematic diagram showing different possible absorption pathways in the stratum corneum (From Scheuplein and Blank 1971).

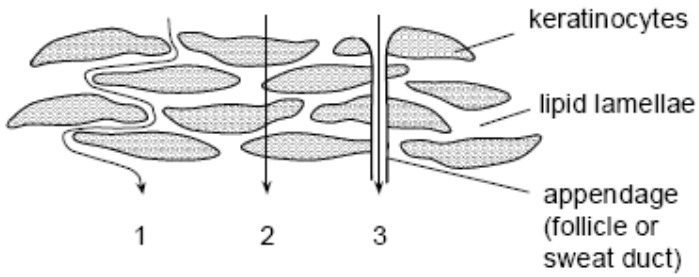

1 = intercellular pathway 2 = transcellular pathway 3 = follicular pathway

Regardless of the exact transport route, it is known that a molecule needs to usually have certain physicochemical properties in order for it to likely penetrate through the skin at a reasonable rate. The properties include; a molecular weight of less than 500 Da; a pKa value between 6 to 9; a melting point below 200°C; and an intermediate lipid-water partition coefficient (Barry, 2001; Meidan and Michniak, 2004).

1.3.3 Factors influencing Transdermal Drug Permeation

Very many variables can control and influence the rate of drug absorption through skin. These can be classified into drug and formulation related factors, physical conditions as well as biological aspects.

1.3.3.1 Drug and formulation-related factors

The drug's aqueous solubility is a major factor and one general rule for transdermal delivery is that the drug should have a higher desirability toward the skin than the vehicle in order to easily transfer into the skin (Barry, 1983). However, it has been estimated that poorly aqueous soluble drugs represent more than half of all drug candidates (Merisko-Liversidge, 2002) so many methods have been used to alleviate this problem such as the use of non-aqueous vehicles. Alternatively, since many drugs are weak acids or weak bases, altering the formulation pH will affect the drug's ionisation status and this will change its solubility. The skin can tolerate a pH ranging from 3 to 9 (Sznitowska et al., 2001).

Another factor is drug concentration as drug flux increases with rising drug concentration. The idea of increasing drug flux by increasing the drug concentration beyond the saturation solubility is termed supersaturation and numerous investigations into this approach have been conducted (Williams and Barry, 2004; Leveque et al., 2006).

Skin hydration is another important variable since as mentioned before the stratum corneum can absorb relatively large amounts of water. The use of transdermal drug delivery patches can act as an occlusive coat, stopping sweat loss and causing skin hydration. Also, any free water present in the stratum corneum may change the drug's solubility in the tissue thus enhancing its partitioning from the vehicle to skin (Williams and Barry, 2004). Hydration will increase drug diffusivity, sometimes to a very large extent (Doukas and Kollias, 2004). In vivo, hydration caused by the

formulation can produce local irritation, reduce patient compliance and cause problems in obtaining regulatory approval for the formulation (Bucks and Maiback, 1999). The skin's hydration status is crucial for hydrophilic drugs and to a lesser extent for lipophilic drugs (Williams and Barry, 2004).

Due to the relatively low permeability of the skin to drugs, chemical penetration enhancers may be incorporated into formulations in order to improve drug penetration. Chemical enhancers include various classes of compounds such pyrollidones, fatty acids, surfactants, urea and terpenes among many others. Penetration enhancers may promote the absorption of drug molecules into the skin by altering the packing of the lipid bilayers in the stratum corneum and thus raising the drug diffusion coefficient. Alternatively, chemical enhancers can change the drug solubility in the skin and influence the partition between the permeant and the skin (Hadgraft 2004).

1.3.3.2 Physical Conditions

The influence of temperature on transdermal drug penetration has been established mostly from in vitro studies. Temperature increases will enhance drug absorption by several different mechanisms. Firstly, heat will directly increase drug diffusivity according to thermodynamic physical laws. For example, an early investigation showed that for a series of n-alcohols, a 5ºC rise in temperature produced an approximate 1.5-fold increase in drug penetration (Blank and Scheuplein, 1969). A temperature rise may also change the intercellular packing of stratum corneum lipids, allowing faster drug diffusion. Heating will also increase in vivo systemic drug

delivery by increasing blood flow although this will only be of significant impact for drugs that rapidly permeate through the stratum corneum (Riviere, 1993). The relative humidity in the environment can affect skin hydration in the manner discussed above.

1.3.3.3 Biological tissue-related factors

It is generally accepted that there are large regional or anatomic site-related differences in skin barrier function. For example, it is known that the skin barrier in the upper arm is about four times greater than that of the forehead (Schaefer and Redelmeier, 1996). There are many reasons for such site-related variations although these are still not fully understood to date. Factors such as keratinocyte surface area, size or composition, number of keratinocyte layers, stratum corneum thickness, intercellular lipid chemistry, the presence of sebum, hair follicle density and dermal blood supply might play a role.

There are also differences between individuals although these have been difficult to estimate. A recent retrospective analysis of 2400 split-thickness skin samples obtained from 112 females involved comparing and analyzing in vitro tritiated water flux data (Meidan and Roper, 2008). It was found that the 112 water flux values were normally distributed and that the coefficient of variation was about 38 %. However, there is strong evidence that variation may be drug-specific so the topic is actually quite complex. There do not appear to be major differences in skin permeability that are related to gender or race. The effect of age is still controversial and less clear with somewhat conflicting results published by different investigators.

Lastly, it should be mentioned that most skin diseases and disorders will have the effect of permeabilising the skin. The exceptions are those conditions that make skin thicker such as calluses, corns and icthyosis.

1.3.4 Physical Methods of Enhancement

Physical methods of enhancing transdermal drug delivery mainly address the problems associated with the delivery of large molecular weight drug molecules such as peptides, small proteins, oligonucleotides or heparins. Physical techniques include iontophoresis, electroporation and microneedles (Meidan and Michniak, 2004). These methods all work using different mechanisms. Iontophoresis works by using low current/voltage electrostatic repulsion to transdermally drive the drug as well as electroosmosis. Electroporation involves use of brief high voltage electrical pulses to cause rapid permeabilisation of the stratum corneum. This can allow large and small peptides as well as other drugs to pass through the skin. The microneedle technique produces transient holes in the stratum corneum. Since the nerves exist much deeper in the skin, the technnique is painless for the recipient (Meidan and Michniak, 2004). A fourth physical technique is sonophoresis, which was used in the current project and is reviewed in the next section.

1.4 SONOPHORESIS FOR DRUG TRANSFER ENHANCEMENT

1.4.1 Background

Sonophoresis describes the use of low frequency ultrasound to transfer low and high molecular weight drugs through skin tissue for either systemic or local therapy (Rao and Nanda, 2009). The technique was first identified in the early 1990s. An early in vivo study (Tachibana and Tachibana, 1991) showed that 48kHz ultrasound allowed significant transdermal insulin penetration in hairless rats. In these experiments, the rats were immersed in beakers filled with insulin solution (20 U/ml) and subjected to ultrasound. It was found that their blood glucose levels halved in 4 hours. Exposure of hairless rats to 48 kHz ultrasound could also lengthen the duration of anesthesia produced by topical lidocaine treatment (Tachibana and Tachibana, 1993). Later research (Tachibana, 1992) showed that low frequency ultrasound could allow transdermal insulin absorption in rabbits. Many subsequent studies confirmed that low frequency ultrasound (less than 100 kHz) was very effective at enhancing the dermal absorption of many different drug molecules. These have included; caffeine (Boucaud et al., 2001), clobetasol-17-propionate (Fang et al., 1999), cyclosporine (Santoianni et al. 2004), fentanyl (Boucaud et al., 2001), mannitol (Merino et al., 2003), morphine (Monti et al., 2001) as well as many others. The number of compounds that have been effectively delivered by means of sonophoresis is continually increasing (Park et al., 2007).

1.4.2 Changes to the Skin

Crucially, low frequency ultrasound does not appear to be damaging to the skin in most cases. For instance, one group (Cantrell et al., 2000) showed that administration of 20 kHz ultrasound at 3.16 W/cm^2 to hairless rats in vivo did not affect keratinocyte morphology. Experiments were also done using 20 kHz ultrasound on human skin tissue in vitro (Boucaud *et al.* 2001). At intensities below 2.5 W/cm^2, no structural changes developed but these did occur at intensities higher than 4 W/cm^2. In other in vitro studies (Mitragotri et al., 1996), no structural changes were observed in human skin following 20kHz ultrasound treatment. Kost et al., (2000) reported that very short applications of 20kHz ultrasound were well-tolerated in humans. On the other hand, others found that low frequency ultrasound can cause skin tissue alterations. For example, Yamashita et al., (1997) conducted human skin in vitro studies and observed some slight detachment of keratinocytes around hair follicles following 5 minutes of 48kHz ultrasound application. In one study (Alvarez-Roman et al., 2003), infrared spectroscopy was used to measure the lipid amounts removed from pig stratum corneum. It was found that a 2 hour exposure to 20 kHz ultrasound released about 30% of all intercellular lipids.

It is important to mention that there is evidence that skin changes caused by sonophoresis are reversible with the skin barrier recovering some time after treatment. Mitragotri and Kost (2000) applied pulsed 20 kHz ultrasound at an intensity of 1.6 W/cm^2 to hairless rats in vivo and measured inulin flux. After 90 minutes of sonication, inulin flux increased approximately 21-times. However, inulin penetration fell to almost baseline levels after the ultrasound was switched off.

Also, 30 minutes application of ultrasound at different frequencies (41, 158, and 445 kHz) to hairless rats caused increased calcein flux by 22.3-, 6.3- and 3.8-fold respectively. Yet once the ultrasound was turned off, calcein permeation returned to its original levels (Mutoh et al., 2003).

1.4.3 Sonophoresis in Human Subjects

The extent of reported transport enhancement produced by sonophoresis has been extremely variable and depends upon the skin species and experimental set up used for the research. It is obvious that the most reliable results are those obtained from human volunteer studies In a double-blind study of 42 volunteers, skin was sonicated at 55 kHz for 10 seconds and a local anesthetic cream was then applied to the skin site for fixed time periods (Katz et al., 2004). The skin was then pricked with a needle. Pain scores and evaluated patient preferences for each treatment were recorded. It was found that ultrasound application significantly improved the local anesthesia effect in the subjects, with the effects starting as early as 5 minutes. In a study of 30 volunteers with alopecia areata, Santoianni *et al*. (2004) showed that 25 kHz ultrasound at an intensity of 0.05 to 0.1 W/cm^2 could enhance methylprednisolone and cyclosporin absorption into skin.

The relative safety of sonophoresis in humans is evidenced by the fact that a dedicated FDA-approved device, called SonoPrep® now exists. The SonoPrep® instrument is a compact, lightweight, battery-operated unit and emits 55kHz ultrasound. It is supplied by Echo Therapeutics (Franklin MA). It has an integrated skin impedance feedback mechanism. An internal sensor measures alterations in

electrical skin impedance during ultrasound treatment and stops the energy when a desired impedance value is reached. Since electrical impedance is related to skin permeability, feedback stops the skin being overexposed to ultrasound.

1.4.4 Mechanisms

1.4.4.1 Cavitation

Cavitation describes a broad range of bubble effects that are caused by pressure changes occurring in an ultrasonicated medium. Cavitation can easily be seen when a transducer emitting low frequency, high intensity ultrasound is immersed in water. Cavitation is observed as bubbles forming near the transducer (Tezel and Mitragotri, 2003). The development of cavitation varies inversely with ultrasound frequency and directly with intensity (Williams et al., 1983). The frequency effect is due to the fact that, at higher frequencies, there is insufficient time for gas molecules to diffuse into growing cavities during the brief rarefaction phase of the acoustic cycle. Hence, gas cavities grow over time. However, the initiation and extent of cavitation is difficult to predict as it depends upon many parameters such as the availability of dissolved gas or surface irregularities that act as nuclei for starting bubble growth.

Over the last 15 years or so, many investigations have been directed towards understanding the mechanisms responsible for sonophoresis. It is now known that permeabilisation is caused mostly by cavitational activity in the stratum corneum. Early evidence for this was provided by Mitragotri et al. (1995b) who used Franz diffusion cell experiments. The researchers passed air through donor and receiver solutions every hour. It was found that this increased the transdermal flux of the

drug molecules used. Since the extent of cavitation is greatly enhanced when dissolved air is present, it was concluded that cavitation was causing enhanced skin permeabilisation. Other proof for a cavitational mechanism comes from the fact that the sonophoresis of mannitol in vitro could be improved by adding porous resins to the donor vehicle (Terahara et al., 2002). Such resins provide more nuclei for gas bubble creation, again showing that cavitation is the mechanism. Also, confirmation for a cavitational mechanism has come from the acoustic spectral analysis. This has indicated that transient cavitation is associated with shock waves caused by symmetrical bubble collapse and high velocity microjets created by asymmetrical bubble collapse (Tezel et al., 2002b).

Recent mathematical modeling indicated that acoustic cavitation can cause air bubbles to grow in the stratum corneum (Lavon et al., 2007). Bubbles join together to create larger bubbles that perturb the tissue. The air escapes when the ultrasound is switched off but the channels created in the stratum corneum remain and these can cross through the entire thickness of the layer. These have been called 'new internal transport routes'.

Whatever the exact cavitational mechanisms, its effects on the epidermal structure have been investigated in several studies (Alvarez-Roman et al., 2003; Paliwal et al., 2006; Wu et al., 1998). In human skin, application of 168 kHz ultrasound created 20μm-diameter air-filled cavities in the stratum corneum lipid bilayers (Wu et al., 1998). The nature of these cavities was consistent with cavitation. Others (Paliwal et al., 2006) used 20nm diameter quantum dots as fluorescent tracers to image pig

epidermis alterations brought about by 20kHz ultrasound. It was reported that ultrasound created or enlarged existing voids in the stratum corneum, creating a 3-D porous network. Tezel et al., (2002a) have developed mathematical models that describe drug transport through such networks.

Since ultrasound induces proportionally more cavitational activity at lower frequencies (Williams, 1983), a consequence is that enhancement increases with decreasing ultrasound frequency. This has been shown in many studies. For example, Mutoh and co-workers (2003) investigated the sonophoretic transport of calcein across hairless rat skin. They used beams of different frequencies (41, 158, and 445 kHz) but all exhibiting intensities of 0.06W/cm^2. Following 30 minutes of ultrasonication, the calcein flux increased by 22.3-, 6.3- and 3.8-fold for frequencies of 41, 158, and 445 kHz, respectively. Sonophoretic enhancement also increases with increasing intensity and application times and this has been shown in many different studies, such as Mitragotri et al., (1996).

1.4.4.2 Heating

Although cavitation is known to be the major mechanism, secondary heating effects can partially contribute to sonophoresis. In a study (Merino et al., 2003), 20kHz ultrasound was used to improve mannitol transport through full-thickness pig skin in vitro. The group used a special control application that did not emit any ultrasound but replicated quite well the heating effects of the beam. The authors found that approximately a quarter of the transport enhancement was caused by higher temperatures but that the rest was due to other mechanisms, probably cavitation.

1.4.5 Enhanced Transport of Macromolecules

There has been considerable interest in recent years over using sonophoresis to deliver therapeutic macromolecules across the skin As already mentioned, positive findings were published in the early 1990s for insulin delivery in rats (Tachibana and Tachibana, 1991) and rabbits (Tachibana, 1992). Important research was performed by Mitragotri et al (1995) who exposed human cadaver skin in vitro to pulses of 20kHz ultrasound at 0.125 W/cm^2. It was shown that ultrasound enhanced the transdermal flux of insulin, γ-interferon, and erythropoietin. In other studies (Mitragotri et al., 1995), diabetic hairless rats were treated with topical insulin while exposed to a 20kHz pulsed beam at 0.225 W/cm^2. These treatments halved the animals' blood glucose level 30 minutes and caused changes in plasma insulin levels. Low frequency sonophoresis of insulin was also reported in hairless rats (Boucaud et al. 2002). Recently, the possibility of transdermal insulin delivery was shown in pigs in vivo (Park et al., 2007). A 1 hour application of very low intensity ultrasound at 20kHz was enough to cause a large drop in the pigs' blood glucose levels. The company, Encapsulation Systems (Havertown, PA), is now performing clinical trials for an insulin delivery using sonophoresis (Kushner et al., 2008). Low frequency ultrasound was also used to permeabilize the stratum corneum to heparin and low molecular weight heparin (Mitragotri and Kost, 2001). Sonophoretic transport of a vaccine and immunological adjuvant was also reported (Tezel at al., 2005).

1.5 AIMS OF THE PRESENT STUDY

The aim of the current study was to explore ways of using low frequency ultrasound to deliver a model macromolecule across full-thickness skin in vitro. The molecule, interferon-gamma, was selected as the model macromolecule since it has a large molecular weight (17000 Da) and it can readily and accurately assayed using a sandwich ELISA method. Full-thickness pig skin was used to model human skin as it is recognised that this skin species is the closest to that of human skin in terms of permeability properties. Different periods of ultrasound application were investigated. Also, the effect of co-application of chemical enhancers with ultrasound was also examined.

The next Chapter (Chapter 2) describes the ultrasound generator and transducer used in this project together with some calibration measurements undertaken on this equipment. This chapter also reviews the basics of generation and propagation of ultrasound and its associated physical properties. Chapter 3 deals with the actual transport experiments used in this project and the findings obtained. The final chapter, Chapter 4, outlines the conclusions from all this work.

CHAPTER 2: THE NATURE OF ULTRASOUND AND ITS CALIBRATION

2.1 INTRODUCTION

This chapter begins by discussing the basic nature of ultrasound, the way it is generated and the means by which it propagates. This is followed by a description of the techniques that can be used to measure and characterise it. Subsequently, there is a description of the ultrasound generator used in this project. The next section describes the various measurements that were used to validate the ultrasonic outputs of this device. The next section deals with the results of the validation studies. Finally, the conclusions section summarises the main ideas developed in this chapter.

2.1.1 The Basic Nature of Ultrasound

Ultrasound is made up of longtitudinal compression waves having a frequency that is too high for humans to hear *i.e.* ≥0.020 MHz (20 kHz). As a result, ultrasound compresses and expands the medium through which it is passing, causing associated pressure changes. Ultrasound is usually created by a piezoelectric transducer that converts electrical energy to ultrasound. Piezoelectricity describes the behaviour of certain materials that expand or contract in response and in correspondence to the voltage that is applied to them. Traditional piezoelectric materials have included ceramic materials such as lead zirconate-titanate, barium titanate or crystalline quartz. However, over the last 30 years, piezoelectric transducers have been increasingly made from new plastics like polyvinylidene difluoride (pvdf), which

maintain their piezoelectric characteristics at temperatures of up to 100ºC (Chivers, 1991).

An important parameter of ultrasound is frequency. This is defined as the number of wavelengths which pass any given point in one second (Williams, 1983). It is usually measured in units of MHz or kHz. The frequency of the ultrasound wave usually depends upon the size of the piezoelectric crystal that generated it.

For continuous wave ultrasound generation, an alternating voltage with a certain frequency is applied to the transducer. This produces continuous wave ultrasound release at the same frequency. To make pulsed ultrasound, short bursts of alternating voltage are repeatedly applied to the transducer. Pulsed ultrasound is usually described as having a certain percentage duty cycle. So for example, if every 1s of ultrasound 'on-time' is followed by 9s of 'off-time' (ie no ultrasound) then the ultrasound is said to have a 10% duty cycle.

It is important to note that once generated, the ultrasound keeps its specific waveform and frequency regardless of the medium it is going through. Another important fact is that ultrasound travels at the same velocity through any single material. Yet velocities often differ between different materials. Table 2.1 lists ultrasound velocities in some different media.

The velocity, frequency and wavelength are interrelated according to the relationship:

$$v = f\lambda \tag{2.1}$$

Where v is the velocity (in m s^{-1}), f is the frequency (in Hz) and λ is the wavelength (in m). Since the frequency remains constant but the velocity varies as the ultrasound travels from one medium to another, this means that the wavelength must also change.

Table 2.1: Ultrasound Velocity in Different Media (from Williams, 1983)

Medium	**Ultrasound Velocity (m s^{-1})**
Air	331
Skin	1500
Water	1500
PMMA ('Perspex')	2680
Brass	4700
Crown Glass	5100
Stainless Steel (347)	5790
Aluminium	6420

In the studies used in our project, ultrasound of frequency 20 kHz was used throughout. By using eq. (2.1), it can be calculated that its wavelength, as it propagated through water or skin were 75 mm.

Another important parameter is the energy of an ultrasound wave as it passes through any point. This is usually expressed in terms of its intensity at that point. Intensity is the power exerted through an imaginary plane orientated at right angles to the direction of wave propagation i.e.

$$I = \frac{P}{A} \tag{2.2}$$

Where, I is the intensity (in W/cm^2), P is the beam power (in W) and A is the area of the imaginary plane (in cm^2).

The pressure exerted by the ultrasound is then given by:

$$p = \sqrt{I\rho c} \tag{2.3}$$

Where p is the acoustic pressure (in Pa), I is the intensity (in W/cm^2), ρ is the medium density medium (in kg m^{-3}) and c is the velocity of sound (in m s^{-1}).

Since intensity may not be evenly distributed in space or in time (in the case of pulsed ultrasound), several different intensity parameters have been defined. The spatial-average temporal-average (SATA) intensity is most commonly used. It is determined by dividing the total power of a beam by its area and, in the case of pulsed ultrasound, averaging over the pulse repetition cycle. However, under certain conditions, much greater ultrasound intensities may develop. Consequently, a spatial-peak temporal-average (SPTA) intensity parameter has been defined. This is the maximum value of the time-averaged intensity within the beam. Also, since the transducer can emit time-dependent fluctuations in intensity, a spatial-average temporal-peak (SATP) intensity parameter exists.

When ultrasound reflects back along its own path, it interferes with that part of itself which has not yet been reflected to create a standing wave. A standing wave has a regular repeating pattern of nodes (where the displacement is zero) and antinodes (where the displacement varies from positive to negative at the same frequency as the incoming wave, but at twice its amplitude). A partial standing wave develops if the reflecting surface is less than 100% effective. *In vivo*, standing wave effects can develop at a boundary between bone and soft tissue. Standing waves can also occur *in vitro,* within Franz-type diffusion cells such as between steel mesh and aqueous solutions (Meidan et al., 1998). Table 2.2 shows the reflectivity of different materials in water.

Table 2.2: The intensity reflectivity of some commonly-used materials in water. The data was obtained from (Chivers, 1991)

Material	**$\text{Intensity}_{\text{reflected}}$ / $\text{Intensity}_{\text{incident}}$**
Air	1.00
Water	0
Skin	< 0.01
Castor Oil	0.02
PMMA('Perspex')	0.37
Crown Glass	0.59
Aluminium	0.85
Brass	0.93
Stainless Steel (347)	0.94

2.1.2 Ultrasound Calibration Methods

A large number of physical technologies and approaches are available for making sure that the values indicated on the ultrasound-generator's control panel actually correspond to the real output of the transducer. The techniques of optical interferometry and capacitance probe measurements are both based on the movement of ultrasound-sensitive membranes. Radiation force-based methodologies are very important and have been extensively used for many years (Preston, 1991). Laser vibrometry is an extremely sophisticated and important approach. However, hydrophones and calorimetric methods were used in the present study and the concept behind each of these is discussed below.

2.1.2.1 Hydrophones

Hydrophones are tiny piezoelectric transducers that work in reverse, converting the ultrasound back to corresponding electrical voltage signals that can be measured and analysed. Hydrophones are very small compared with the ultrasonic wavelength and exhibit resonant frequencies much greater than the beam being measured. Hydrophones are mostly used for beam plots but are also effective for determining various aspects such as; the absolute intensity at a point, the ratio of peak to average intensity, and identifying the size and location of high intensity spots within the beam (Williams, 1983). Hydrophone design is very application-specific and depends upon the frequency being measured and the medium of operation.

2.1.2.2 Calorimetric Methods

As ultrasound propagates through a medium, its intensity falls exponentially as a result of attenuation and absorption (Williams, 1983). In a uniform medium, where scattering is usually negligible, absorption is caused by viscosity, molecular relaxation or thermal conductivity mechanisms. These produce a temperature rise whose measurement is the basis of the calorimetric approach. The approach assumes that all of the ultrasound energy is converted to heat (Teo et al., 2001). The calorimetric approach is an easy and convenient method that can be used on a daily basis in laboratories to measure the absolute acoustic energy delivered in different systems (Kimura et al., 1996). Its disadvantage is that it only measures total power and provides no information on space-dependent or time-dependent variations.

2.2 CALIBRATION OF THE ULTRASOUND SOURCE

2.2.1 The Ultrasound Generator Used in These Studies

Figure 2.1: The ultrasound generator used in the current project (from: www.sonicsandmaterials.com)

A 20 kHz ultrasound generator (VCX-5000) was used to generate the ultrasound for all the experiments undertaken in our project. This instrument was bought from Sonics & Materials (Newtown, CT) and includes a generator plus connecting transducer probe of 3 mm diameter. Fig. 2.1 shows a photograph of the equipment although we used a much smaller 3mm-diameter transducer unlike the larger one shown. The VCX-500 generator has inbuilt features such as a digital display of the power that is being delivered to the transducer. The instrument also has an integrated temperature controller, process timer and pulse-generator. The temperature control feature prevents dangerous overheating by stopping the ultrasound when the sample temperature reaches a certain limit. The function of the process timer is to modulate total processing time (1 second to 10 hours). The function of the on/off pulser is to

create independent pulses of ultrasound, each lasting from 1 second to up to 59 seconds.

We decided to initially check the ultrasonic accuracy of the VCX-500 generator. This is because many studies have shown that is often the case that the actual output characteristics of a device may not match the manufacturer's claimed values (Meidan et al., 1995; Meidan et al., 1998). Validation was done with respect to the frequency and the intensity.

2.2.2 Frequency Measurements

Frequency validation was done by our collaborators at the Centre for Ultrasonic Engineering (CUE) at Strathclyde University. The method required use of a regular hydrophone (B&K 8103, Stevenage, UK) directly connected to an Infinitum Megazoom oscilloscope (Agilent, Wokingham, UK) operating at 500MHz and 2GSa/s. We found that a major problem was that the VCX-500 generates cavitation. Actually, even at the lowest amplitude setting, the emitted ultrasound produced enough cavitation to prevent the operation of the hydrophone. This difficulty was overcome by controlling the processor using an external DC voltage source connected through a 9-pin D-type socket. This was used to lower the amplitude setting to 5% where no cavitation seemed to occur. Both the transducer and hydrophone were immersed in a 5-litre tank filled with distilled water. Since the emitted ultrasound was below the intensity threshold, no de-gassing of this water was necessary. Acoustic pressure oscillations were measured at a distance of 5 cm from the transducer face. The arrangement used is shown below in Fig.2.2.

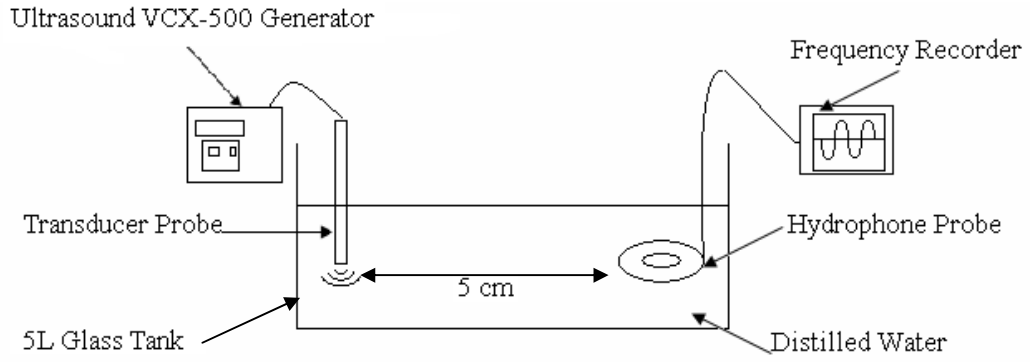

Figure 2.2: Diagram showing the arrangement used to measure ultrasound frequency

2.2.3 Intensity Measurements

According to the manufacturer, the ultrasound intensity emitted by the transducer could be determined by doing a simple procedure. This method involved switching on the ultrasound and adjusting the processor's amplitude dial to a selected value ranging from 21% to 40%. In practice, values of 21%, 25%, 30% and 35% were selected. In all cases, the transducer was immersed in a 500 ml beaker of water and the wattage displayed on the power monitor was recorded. Without changing the amplitude setting, the transducer was repositioned so as to operate in the air. Again, the amount of watts displayed on the power monitor was recorded. The difference between the two wattage readings was divided by the transducer area in order to obtain the manufacturer's intensity value. The measurements were performed three times for each chosen amplitude setting.

In order to independently check these values, we used a simple home-made calorimetric approach (Kimura et al., 1996; Merino et al., 2003) developed in our laboratory. For this, the transducer was immersed in a Dewar-type (Dilvac®) thermoflask (VWR, Lutterworth, UK), containing 500ml of distilled water. Continuous wave ultrasound was applied for 15 minutes at different amplitude settings. A thermometer was used to measure water temperatures both before and immediately after ultrasound application. The thermometer was always removed when the ultrasound was switched on. Temperature measurements were done in triplicate. Fig. 2.3 provides a schematic diagram of the arrangement used.

The equation below was used to calculate the SATA intensity output:

$$I = \frac{M \times W}{A} \times \Delta T \qquad (2.4)$$

Where I is the ultrasound intensity (W/cm^2), M is the water mass (0.5 kg), W is the heat capacity of water (4.18 J/g °C), ΔT is the temperature change (°C), and A is transducer surface area (0.0707 cm^2).

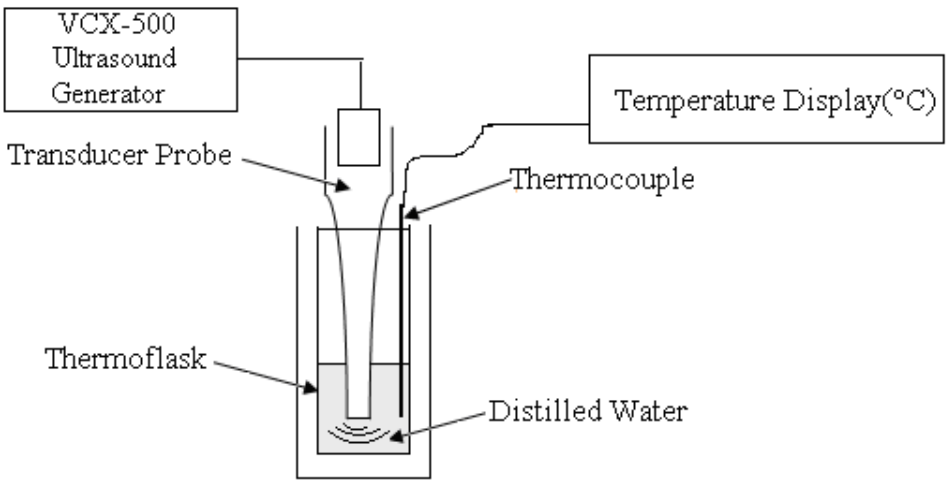

Figure 2.3: Diagram showing a scheme of the apparatus used to measure ultrasound intensity in our laboratory.

2.3. RESULTS AND DISCUSSION

2.3.1 Frequency Check

Hydrophone measurements indicated that the frequency was always 19.88 kHz, which is very close to the manufacturer's value of 20 kHz. Fig. 2.5 shows the waveform detected by the hydrophone. This acoustic signal has a peak-to-peak voltage of 15.4mV. Unfortunately, the software we used did not enable us to incorporate the x- and y-axis scales and noting that the pressure has arbitrary units so it was normalised to the peak pressure which is directly in front of the transducer. From the calibration data for the hydrophone, the acoustic pressure was calculated to be approximately 500kPa.

Figure 2.5: The detected acoustic signal

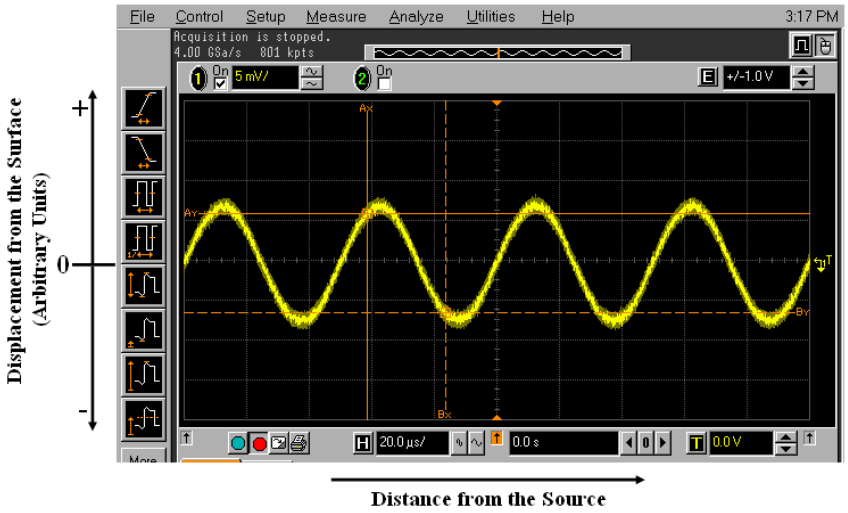

2.3.2 Intensity Check

From the manufacturer's specified method, it was found that there was a good linear relationship between the % amplitude setting and the measured intensity (r^2= 0.97). The data is shown below in Fig. 2.6. It should be mentioned that the processor's maximum amplitude was below 40%.

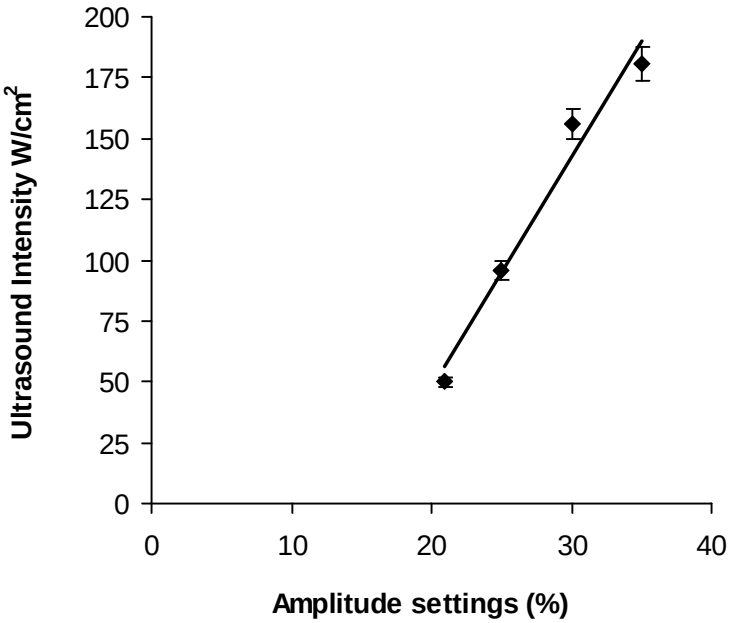

Figure 2.6: Intensity as a function of the amplitude setting as determined by the manufacturer's method. Error bars show standard deviation values. n=3.

In order to verify the output measured by the manufacturer's preferred method, we run our own calorimetric measurements of intensity. See Fig. 2.7. These showed that the recorded temperatures rose linearly with increasing amplitude (r^2=0.99). Then, these recorded temperature increases were converted into ultrasound intensity values using the equation (2.4). Fig 2.8 shows the resulting graph that was obtained.

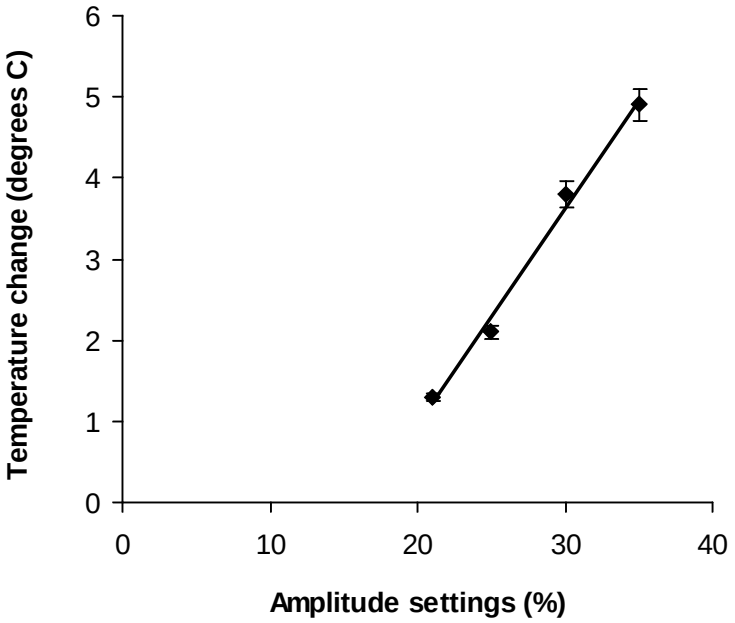

Figure 2.7: Temperature change as a function of amplitude setting as determined from our calorimetric measurements. Error bars show standard deviation values. n=3.

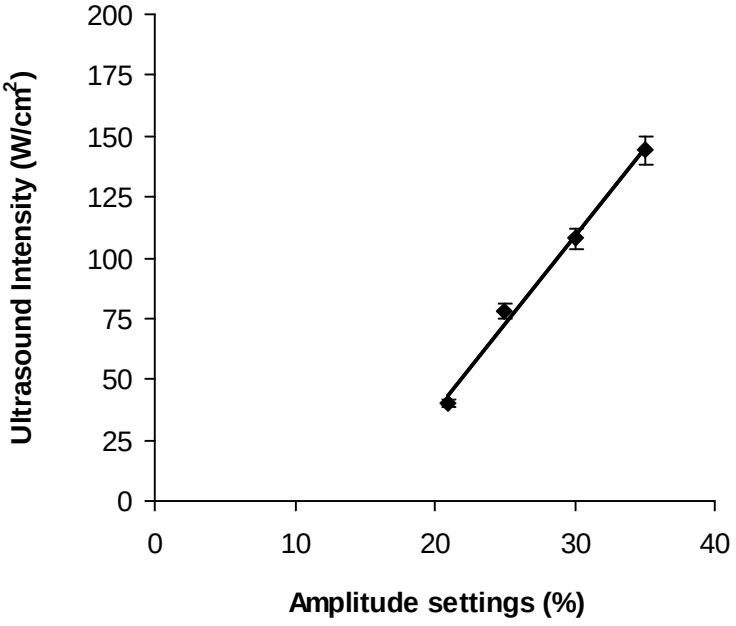

Figure 2.8: Intensity as a function of the amplitude setting as determined by the calorimetric method. Error bars show standard deviation values. n=3.

Fig. 2.9 shows a graph relating the intensities as measured by the two different methods.

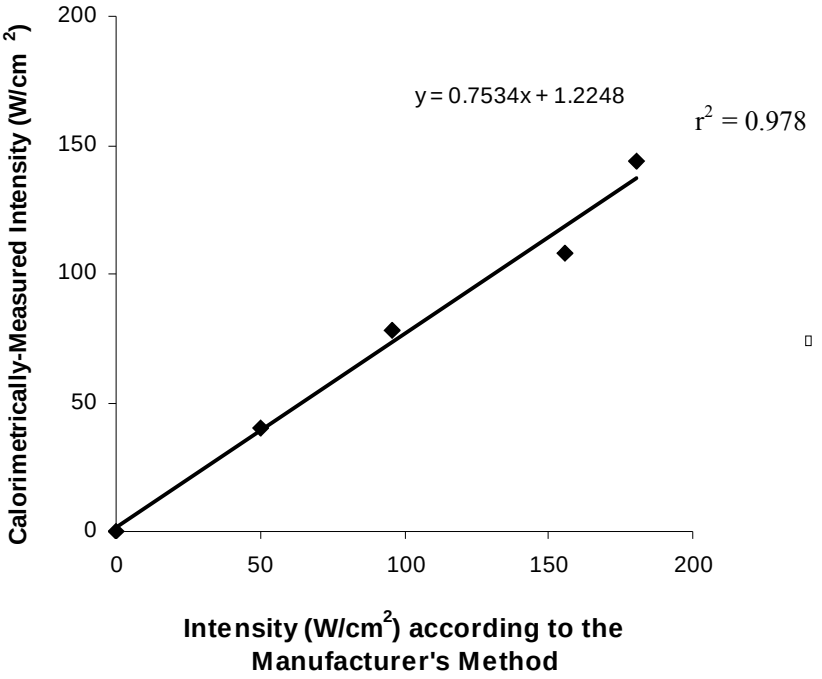

Figure 2.9: Intensity calibration plot for the VCX-500 ultrasound generator. n=3

It can be seen that the calorimetrically-measured intensities were lower (~25%) than that measured according to the manufacturer's method. Part of the reason for this might be that not all of the energy was being converted into heat as some was creating cavitation, microstreaming and mechanical effects in the water. Also, the generator may have lost some efficiency in the 4 year period since it was first purchased. However, the calorimetric measurements were rerun about every 2 months in order to ensure that the generator was operating correctly throughout the project. These re-measurements showed the instrument's output was consistent over

long time periods and it therefore it could be used as an ultrasound source in these studies.

2.4 CONCLUSION

Measurements of the transducer operating frequency showed that the actual frequency was very close (-0.6%) to the 20kHz value claimed by the manufacturer. With regards to intensity, the manufacturer's suggested method was checked against our own calorimetric method. The calorimetrically-measured emitted intensities was somewhat lower (~25%) than that measured by the manufacturer's method. However, the output was always consistent over time and the response increased in a linear manner with the amplitude setting on the equipment's dial. In conclusion, the VCX-500 generator and transducer were suitable for using as an ultrasound source in our present sonophoresis project.

CHAPTER 3: INTERFERON-GAMMA TRANSPORT STUDIES

3.1 INTRODUCTION

This chapter deals mostly with the in vitro permeation studies that were run as part of the investigation into sonophoresis. Full-thickness porcine skin was used to model human skin since it is established that this skin species is the closest to that of human skin in terms of permeability characteristics (Godin and Touitou, 2007; Frum et al., 2008). Moreover, this skin is cheaper, much more readily-sourced and requires less regulatory approval than human skin. Full-thickness skin was used as this is probably much more representative of the in vivo situation than split-thickness skin, epidermal membranes or trypsinised stratum corneum samples. In the in vitro transport experiments, the variables investigated were different durations of ultrasound application as well as the effect of pretreatments with different chemical enhancers.

Since the literature relating to transdermal drug delivery, sonophoresis and ultrasound acoustics have already been described, the rest of this section deals with interferon-gamma, (the selected model macromolecule) as well as the different chemical enhancers used as skin pretreatments. There then follows a Methods section that describes the modified Franz diffusion system that was used to run the permeation studies. Ultrasound exposure was done under conditions that caused very little skin surface heating. The final sections describe the transport data obtained and summarises the important findings of this research.

3.1.1 Interferon-gamma

Human interferon-gamma is a dimerised, soluble cytokine with a molecular weight of about 17000 Da. It is important immunologically for the innate and adaptive immunity it can give against viral and intracellular bacterial infections as well as for certain forms of tumor control. Although this cytokine has been used therapeutically to treat various cancers (Hastie et al., 2008), in this project it is being used simply as a model macromolecular drug. Its large molecular weight and the relative ease that it can be assayed by means of a ready-available sandwich Enzyme-linked immunosorbent assay (ELISA) make it useful for this role.

3.1.2 Terpenes

These compounds are naturally-occurring volatile oils that are mostly extracted from certain flowers, fruits, seeds and plant leaves. For example, carvone is extracted from caraway seeds. Terpene molecules are made up of isoprene (C_5H_8) units and classification is often done according to the number of such units existing in the molecule. Monoterpenes (C_{10}) have two isoprene units, sesquiterpenes (C_{15}) have three units and diterpenes (C_{20}) have four units. Terpenes can also be divided according to their functional groups egs hydrocarbons, ketones or cyclic ethers.

In recent years, considerable interest has been shown in the use of terpenes as penetration enhancers for transdermal delivery systems (Vaddi et al., 2002; Williams and Barry, 2004). Although terpenes have good enhancement capabilities, they usually show low skin irritancy and toxicity, especially at low concentrations such as 1-5% (Williams and Barry 2004;). If any irritation occurs, it is usually short-lasting

(Okabe et al 1990). Also, some terpenes can cause no skin irritation at all. Hence, the FDA in the United States has officially designated terpenes as GRAS, which means 'generally recognized as safe' (Godwin and Michniak, 1999; Asbill and Michniak, 2000).

Importantly, terpenes can increase the percutaneous absorption of both hydrophilic and lipophilic drugs (Williams and Barry, 2004). The lipophilicity of the terpene and the drug is important in determining how much enhancement occurs. Lipophilic hydrocarbon terpenes, such as limonene, are more effective for lipophilic drugs (El-Kattan et al 2001). Hydrophilic terpenes like menthol, which are capable of hydrogen bonding, are usually effective in enhancing the penetration of hydrophilic drugs (Godwin and Michniak 1999; Williams and Barry 2004). In the case of hydrophilic drugs, terpenes increase just drug diffusivity through the skin. For lipophilic drugs, terpenes increase both drug diffusivity and drug partitioning into skin. (El-Kattan et al 2001). Other aspects of terpene structure also affect the extent of enhancement. Terpenes with the least branched structures are usually stronger enhancers, although the exact reasons for this are still unclear. Another structure-specific activity is the long chain sesquiterpene, nerolidol. Its enhancer activity is due to its amphiphilic structure that aligns with the lipid lamellae of the stratum corneum and disrupts its packing arrangement. In general, terpenes seem to be more effective as enhancers when they are formulated in propylene glycol (Vaddi et al., 2002).

There are virtually no reports discussing the combined effect of terpenes and low frequency ultrasound on transdermal drug absorption. The GRAS designation of terpenes means that they probably may be good candidates for combination use with ultrasound if synergism developed. In order to test this, we chose three chemically-dsistinct monocyclic terpenes for use in our drug delivery experiments. These were (+)-carvone (an ether), menthone (a ketone) and terpineol (an alcohol). All these hydrophilic terpenes have a free hydroxyl or oxygen group and so they should be able to disrupt stratum corneum lipid packing through the formation of hydrogen bonds (Vaddi et al., 2002). All these terpenes have a similar density of about 0.9g/ml.

3.1.3 Fatty acids

Fatty acids are a popular group of chemical penetration enhancers (Mittal et al., 2009). These compounds work by opening up the intercellular lipids in the stratum corneum, allowing any applied drug to more readily permeate through the lipid bilayers. The exact mechanisms are not yet fully understood. It is possible that fatty acids can remove some of the endogenous stratum corneum membrane components, allowing phase separation to develop. This will reduce the amounts of crystalline lipids and create more permeable fatty acid-rich domains (Rowat et al., 2006).

In terms of chemical structure, fatty acids consist of an aliphatic hydrocarbon chain and a terminal carboxyl group. They differ from each other in various aspects such as hydrocarbon chain length as well as the number, position and configuration of double bonds. Other differences include the extent of chain branching or the

presence of extra functional groups. The enhancer effect of any given fatty acid is known to be related to its molecular structure. For instance, short chains are not lipophilic enough to allow the fatty acid to enter the stratum corneum while very long chains have too high an affinity to stratum corneum lipids, thereby preventing their own continual permeation and that of other any drug. A medium chain length is usually best. For saturated fatty acids, a hydrophobic chain length of about 12 carbon atoms was found to be optimal, generally possessing a good balance between partition coefficient, solubility and skin affinity (Elyan et al., 1996). For unsaturated fatty acids, chain lengths of about 18 carbon atoms seem to be most effective (Williams and Barry, 2004). Also, the presence of double bonds will affect the effectiveness of any fatty acid as a penetration enhancer. Unsaturated fatty acids are usually stronger enhancers than saturated ones (Mittal et al., 2009).

Given the widespread use of fatty acids as transdermal enhancers, there are actually virtually no published studies dealing with their combined application with low frequency ultrasound. One aspect of the current study was to explore the combination treatment of each of three fatty acids with low frequency ultrasound. The tested fatty acids were linoleic acid, oleic acid and stearic acid. Fig. 3.1 shows their structures. It can be seen that these three molecules differ in the number of unsaturated bonds.

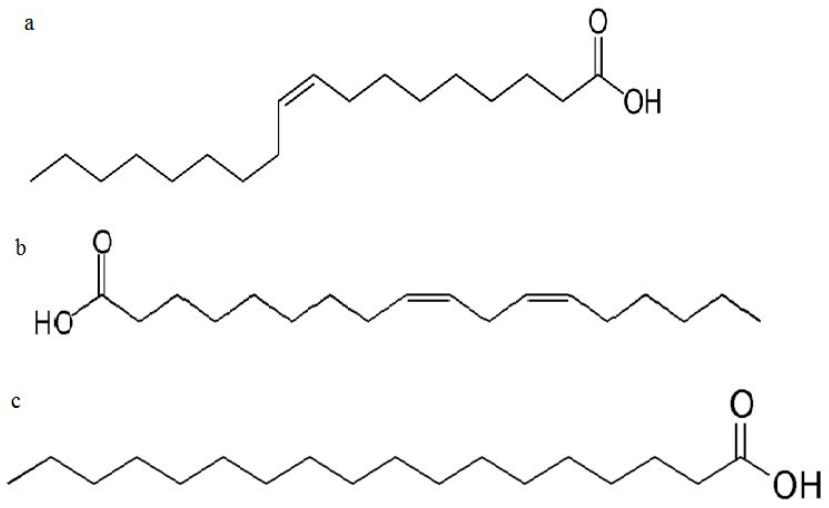

Fig. 3.1: Molecular structure of the fatty acids used in this project. (a) oleic acid, (b) linoleic acid and (c) stearic acid.

3.1.4 Anionic surfactants

At the molecular level, anionic surfactants usually consist of a lipophilic alkyl chain and a hydrophilic, negatively charged head group. Anionic surfactants can affect the skin by interacting with either keratin in the corneocytes or the proteins in the intercellular bilayers (Williams and Barry, 2004). These changes will permeabilise the stratum corneum, allowing more rapid flux of any applied drug compounds. The potency of anionic surfactants seems to be dependent upon the surfactant chain length. Very short chain lengths will result in a molecule exerting very weak surfactant action. However, longer chain lengths will cause the molecule to partition and diffuse through skin too slowly. This is due to the greater molecular weight of

such molecules. A 12-carbon tail group is usually the best in terms of allowing good chemical enhancer effects (Tezel et al., 2002c).

With a chain length of 12 carbon atoms, sodium lauryl sulphate (SLS) has attracted considerable attention as a transdermal enhancer. Fig. 3.2 shows its molecular structure.

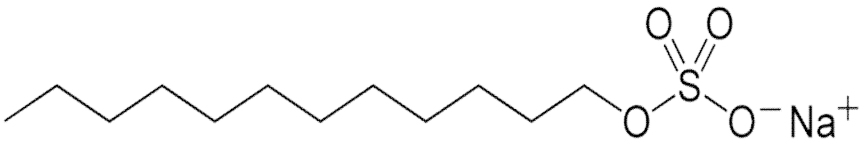

Fig. 3.2: Molecular structure of sodium lauryl sulphate

It is thought that when it is applied to the skin, SLS enhances drug flux through its capacity to uncoil and extend α-keratin in the stratum corneum. Also, migration of SLS into the intercellular lipid bilayers may reduce the ability of lipids to pack together (Wilhelm et al., 1991). All these changes allow higher drug diffusivity rates for all drugs but especially more hydrophilic ones (Borras-Blasco et al., 2004)

SLS is of great interest in relation to sonophoresis as it was already shown to act synergistically with 20kHz ultrasound in enhancing transdermal drug delivery. Mitragotri et al. (2000b) investigated the combining effect of ultrasound with SLS in *in vitro* full thickness pig skins. Mannitol was used as a model drug. Application of SLS alone for 90 minutes produced an approximate 3-fold increase in mannitol permeation, while application of ultrasound alone for 90 min produced an approximate 8-fold enhancement. However, a combination of ultrasound from 1%

SLS solution produced an approximate 200-fold increase in transdermal mannitol flux. SLS treatment also lowered the threshold ultrasound energy needed to induce a measured change in the skin's electrical impedance – a parameter considered proportional to the skin's permeability status. Without surfactant, the threshold ultrasound energy for producing a detectable change in skin impedance was about 141 J/cm^2. Addition of 1% SLS decreased the threshold to only 18 J/cm^2.

In terms of mechanisms, there seem to be contradictory explanations for the effectiveness of the SLS-ultrasound combination. In one study, the authors (Tezel et al., 2002c) observed sulphorhodamine dye penetration through skin samples under the influence of various treatments. Treatments were ultrasound alone, SLS alone, ultrasound with SLS and control conditions. The sulphorhodmaine deposition images indicated that synergism could be due to the 20 kHz ultrasound enhancing SLS dispersion within the skin. On the other hand, Lavon et al., (2005) found that exposure of skin to low frequency ultrasound altered the stratum corneum's pH profile. The authors explained this effect by the ultrasound-induced discharge of acidic by-products – a phenomenon termed sonolysis. These by-products changed the ionization status of SLS and hence its lipophilicity, causing more SLS partitioning and permeation into the skin surface.

In the present study, sonophoresis of the model macromolecule, interferon-gamma, was investigated following pre-treatment with either SLS, sodium octyl sulphate (SOS) or sodium eicosyl sulphate (SES). The latter two have the same structure as SLS except the alkyl chains are only 8 and 20 carbons in length, respectively.

3.2 METHODS

3.2.1 Chemicals

A Human interferon-gamma-Cytoset™ was purchased from Invitrogen (Dorchester, UK). This has all the components and reagents required for running the enzyme-linked immunoassay for specific and quantitative measurement (ELISA) of human interferon gamma. The set included; human interferon-gamma (code: CHC1233), bovine serum albumin fraction 5, as well as the Biosource cytoset™ buffers set (containing buffer A, buffer B, assay solution, Tetramethylbenandzine / hydrogen peroxide substrate solution, stop solution and wash buffer). Sodium lauryl sulphate (SLS), sodium octyl sulphate (SOS), sodium eicosyl sulphate (SES), α-terpineol, (+)-carvone, linoleic acid, oleic acid, stearic acid and phosphate buffer saline (PBS) tablets (pH 7.4) were purchased from Sigma–Aldrich (Poole, UK). Double distilled, de-ionised water was used throughout.

3.2.2 ELISA Assay

Interferon-gamma was assayed by a sandwich ELISA method that involved use of an antibody pair against human interferon-gamma (Walker and Rotondo, 2004). So 96-well NUNC™ microtitre plates, (Thermofisher, Horsham, U.K.) were coated with 2 μg/ml capture monoclonal antibody prepared in PBS (pH 7.4) and incubated for 18 h at 4°C. The wells were then washed 4 times with PBS containing 0.5% (v/v) Tween-20 (PBS/Tween). Then, a sample buffer of PBS containing 0.5% (w/v) bovine serum albumin and 0.1% (v/v) Tween-20 was added to the plates and incubated at room temperature for 2 h. The plates were washed 3 times with PBS/Tween. Subsequently, samples or interferon-gamma standards were added to wells (diluted

in sample buffer). This was followed immediately by the addition of 0.16 μg/ ml biotinylated detection antibody in sample buffer, which was incubated for 2 h at room temperature. After 4 more washes with PBS/Tween, streptavidin horseradish peroxidase-conjugate was added (1:2500 in sample buffer) for 30 minutes at room temperature. The plates were then washed 5 times with PBS/Tween before the addition of 3,3', 5,5'-tetramethyl-benzidine for 30 min. Subsequently, 1M sulphuric was added to stop the reaction and the absorbance at 450 nm was measured on an ELISA plate reader. Interferon-gamma amounts in samples were calculated on each occasion by 3° order polynomial regression using a suitable calibration curve.

3.2.3 Preparation of the Skins

Skin tissue was obtained from pig ears (Landrace species) made available by a local abattoir. The ears were collected immediately after slaughter of the animals but before any steam sterilisation took place. At the labs, the ears were washed in cold running water. Each ear was divided horizontally by scalpel to give whole skin samples, of approximate area 8cm^2. Then, the skins were checked by naked eye to ensure their integrity and that there were no holes in the tissue. The skins were stored at -80˚C for not more than 3 months. Immediately before the transport studies, the skin sections were thawed at room temperature and cut into smaller samples (surface area of about 1cm^2), suitable for inserting into Franz diffusion cells.

3.2.4 Initiation of the Permeation studies

The full-thickness skins were inserted in Franz diffusion cells (PermeGear, Bethlehem PA) with a surface area of 0.64 cm^2 and a receptor cell volume of 5.3 ml.

The receptor solution was PBS at pH 7.4. This solution was stirred at 600rpm and maintained at 37ºC by the use of a thermostatic water pump (Haake DC10, Karlsruhe, Germany) that circulated water through each chamber jacket. The skins were initially allowed to hydrate in the Franz cells for 1 hour. During this time, the cells were occasionally turned upside down in order to allow the escape of any air bubbles that might have developed on the skin underside. Then, in some experiments, the skins were treated with a 0.5 ml application of a selected chemical enhancer solution. This was either 0.5% w/v of SOS, SLS or SES in aqueous solution; 2% v/v menthone, carvone or alpha terpineol in propylene glycol; or 2% w/v lauric acid, linoleic acid or stearic acid in propylene glycol. In all cases, the enhancer solution was left on the skin surface for 1 hour and then removed by pipette. Subsequently, 0.5ml of 0.8% (w/v) interferon-gamma solution prepared in PBS (pH 7.4) was deposited on each skin.

3.2.5 Ultrasound Application Protocol

Ultrasound application was started immediately after loading of the interferon-gamma solution. For this purpose, the transducer of the VCX-500 generator (described in Chapter 2) was fixed into position perpendicular to the skin surface. It was immersed into the donor solution such that its active tip was located approximately 5mm above the skin surface. A pulsed beam with a 10% duty cycle (ie 1s on: 9s off) was used. This had a SATA intensity of 3.7 W/ cm^2. In the anionic surfactant studies, the application time was either: 0 (control), 30, 60, 120, 240 or 300s. In the terpene and fatty acid studies, the application times were either 0 (control) or 300s. Use of pulsed ultrasound used over such brief periods had the

advantage that resulting skin surface temperature increases were small and never exceeding presonication temperatures by more than 3ºC (data not shown). Hence, the methodology was close to what could be applied in a clinical setting where brief applications times that produced little heating were desirable. After sonication, the transducer was removed and the donor cell was sealed with Parafilm®.

It must be stated that a special control experiment was also run in which the receiver solution was exposed only to porcine skins. No cytokine, enhancer or ultrasound was applied. The aim was to determine if this alone caused an ELISA reaction.

3.2.6 Sampling

Drug permeation was allowed to continue for usually 24h. At chosen times, a 100µl volume was withdrawn from each receiver solution and replaced with the same volume of PBS solution to compensate for the volume decrease. The withdrawn interferon-gamma samples were placed in eppendorf tubes and stored at -20ºC until ready for ELISA analysis. Each individual experiment consisted of 4 replicate runs. In all cases, interferon-gamma concentration values obtained for each aliquot were corrected for the progressive dilutions developing during the course of the Franz cell experiment (Khan et al., 2005). This was done by using dedicated Microsoft Excel software on an IBM-compatible computer.

3.2.7 Data Analysis

Data was analysed by using the 2-tailed unpaired students *t*-test with significance set at $P = 0.05$.

3.3. RESULTS

3.3.1 ELISA Calibration Curve

Fig. 3.3 shows the calibration plot obtained for the ELISA immunoassay run in the laboratories. It can be seen that there was a good linear correlation between interferon-gamma concentration and the recorded optical density. Although the line does not pass the origin, this was in fact an expected feature of this immunoassay, as described in the guidelines and information that came with the purchased Cytoset™.

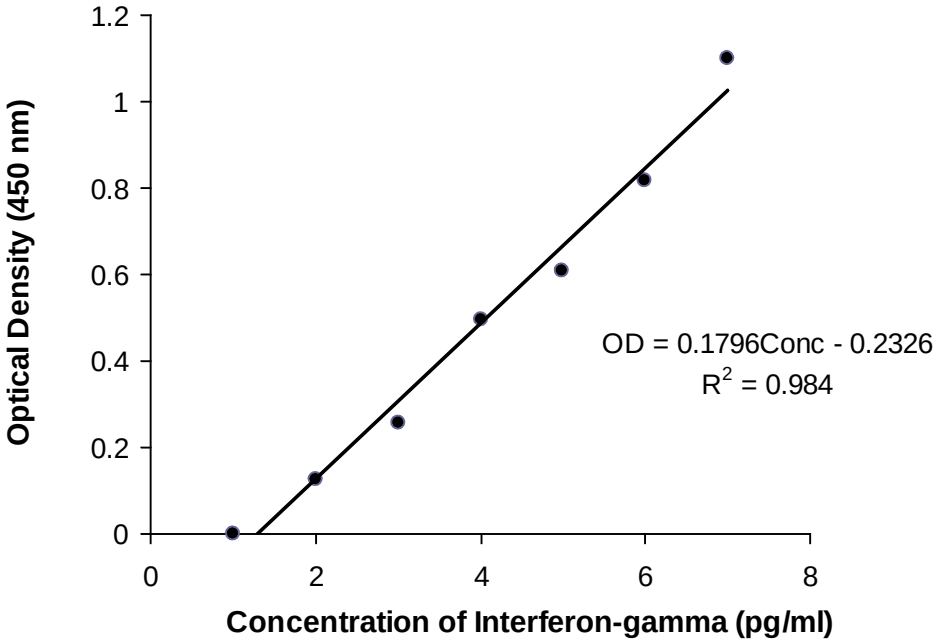

Fig. 3.3: Calibration curve obtained from the interferon-gamma ELISA assay

3.3.2 Effects of Ultrasound and Anionic Surfactants

The special control experiment resulted in no ELISA reaction showing that the assay was not affected by exposure to pig skin residues and was hence suitable for its designated purpose. Fig. 3.4 shows interferon-gamma permeation over 24 hours following different durations of ultrasound application. No chemical enhancers were

used. It can be seen that without ultrasound, the amount of macromolecule that permeated through the skin was negligibly small (≤ 1ng/cm^2).

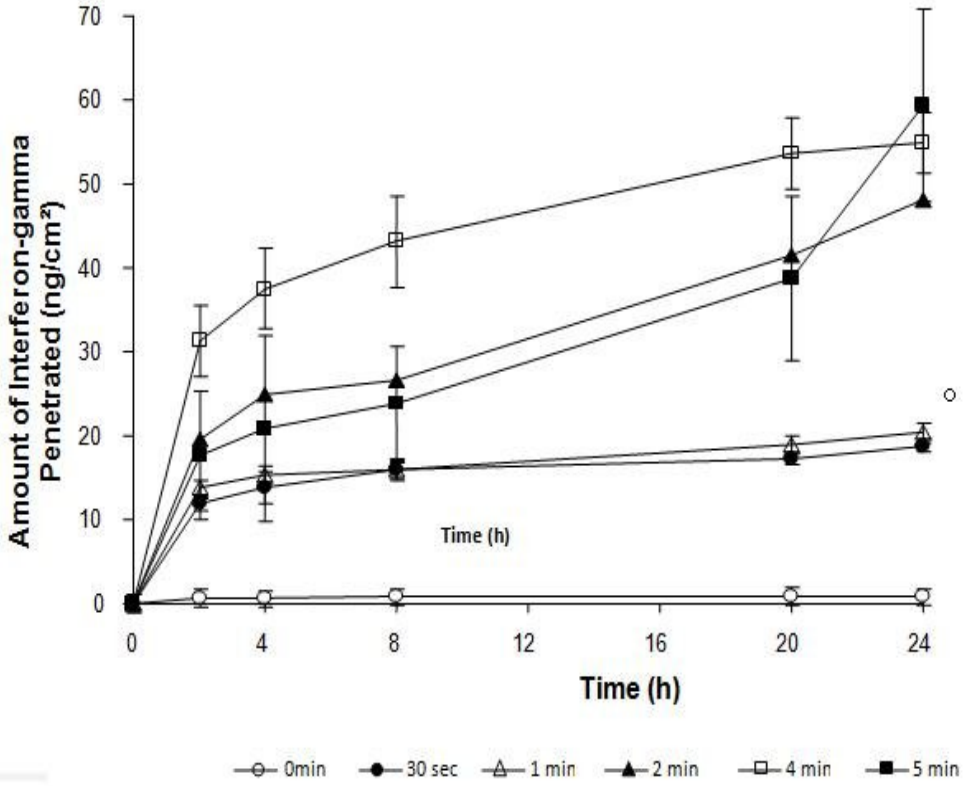

Fig. 3.4: Transdermal penetration profile of interferon-gamma and the influence of different sonication periods. Error bars indicate S.D. values, n=4.

However, application of 30 s of ultrasound caused a sharp initial increase in flux so that about 12ng /cm^2 had permeated through by 2 hours. Then, cytokine flux fell back down so that total amounts permeated at 24 hours (approx. 18 ng /cm^2) were only slightly greater than that at 2 hours. Ultrasound application for 1 minute produced a very similar interferon-gamma permeation profile to that of the 30 second application. Greater durations of ultrasonication of 2, 3 and 5 minutes produced more marked increases in initial macromolecule flux in the first 2 hours. In all three cases, this was then followed by a second almost linear or quasi-linear phase lasting

until 24 hours in which the drug permeated through the pig skin at a reduced rate. Within this overall pattern, there were slight but erratic differences between the permeation profiles following 2, 3 and 5 minutes of ultrasound application. These differences are difficult to explain.

In regards to Fig. 3.4 as a whole, it is important to note that since the amount of interferon gamma in the donor cell was 4mg *i.e.* 4 x 10^6 ng, the amount that could permeate through to the receiver cell under sonophoresis was tiny compared to the total quantity available in the donor cell. Also, sink conditions were maintained throughout and no obvious precipitate could be seen. Therefore, the fact that transdermal flux does not follow the classic lag time followed by steady state profile in all five experiments is challenging to explain. One possible explanation for the fact that in all five experiments, flux actually decreases at certain times relates to the fact that the stratum cornuem is somewhat elastic (Yuna and Verma, 2006). It is possible that some time after the ultrasound is switched off, some cavitationally-created defects or channels in the stratum corneum contract. Such contractions may reduce the flux of large macromolecules like interferon-gamma.

Fig. 3.5 depicts macromolecule permeation following SOS pretreatment followed by sonication for different durations. It can be seen that without ultrasound, SOS treatment caused high drug flux at the start so that the mean amount permeated had reached about 10 ng /cm^2 by 2 hours. Thereafter, the rate of cytokine flux goes down so that the total mean amount permeated by 24 hours was approximately 20 ng /cm^2. Progressively lengthier durations of sonication seem to increase the magnitude of the

sharp initial flux rise. Ultrasound application for 0.5, 1, 2, 4 and 5 minutes caused macromolecule permeation at 2 hours to reach mean levels of approximately 10, 14, 16, 28 and 28 ng/cm^2. However, the duration of ultrasonication did not seem to greatly affect interferon-gamma flux from 2 to 24 hours. Drug flux in this period was always lower than that in the first 2 hours and was more or less constant in most cases, irrespective of ultrasound exposure time. Again, an explanation for observed decreases in flux after 2 hours may be contraction of the stratum corneum defects.

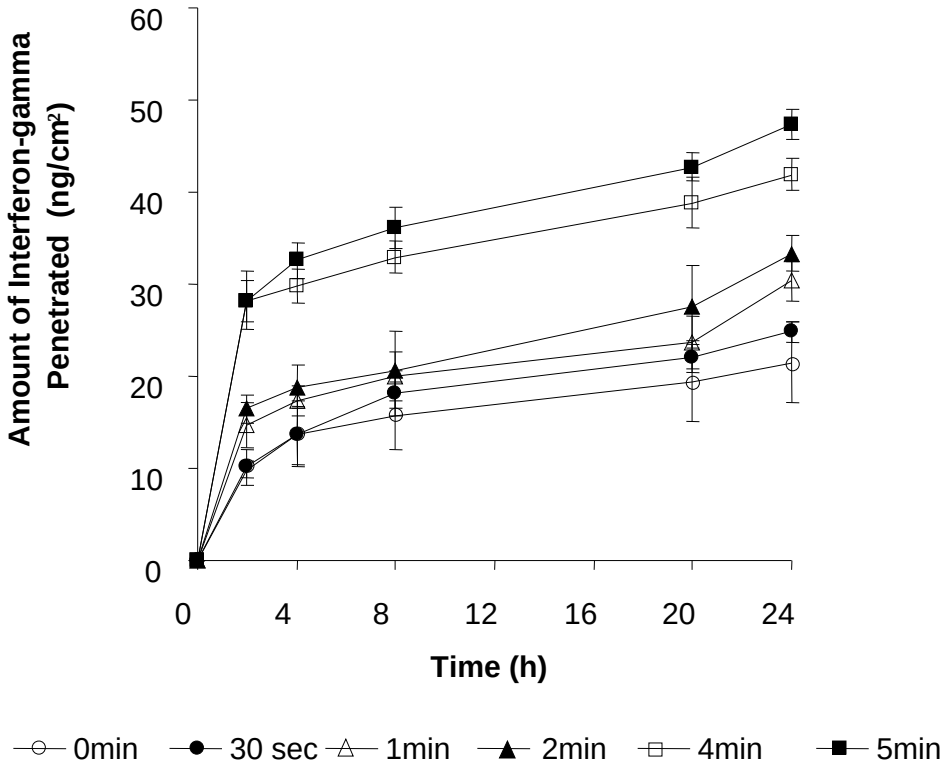

Fig. 3.5: Transdermal penetration profile of interferon-gamma following sodium octyl sulphate pretreatment. Legend symbols refer to different sonication periods. Error bars indicate S.D. values, n=4.

Fig. 3.6 shows the cumulative permeation data for experiments in which the pig skins were pretreated with SLS solution. Without ultrasound, cytokine flux was high at the

start so that the mean amount permeated was approximately 12 ng /cm^2 at 2 hours. In the following hours, transdermal flux rate rapidly decreased so that the total amount permeated averaged about 20 ng /cm^2 at 24 hours. Ultrasonication seemed to increase drug amounts permeation in the first 2 hours. A 5 minute application, the longest, resulted in a mean amount at 2 hours of about 35 ng /cm^2. In contrast to the SOS results, lengthier sonication tended to increase permeation rates over the 2 to 24 hour period too. This might be because the longer alkyl chain of SLS means it is a stronger surfactant causing more stratum corneum lipid disordering.

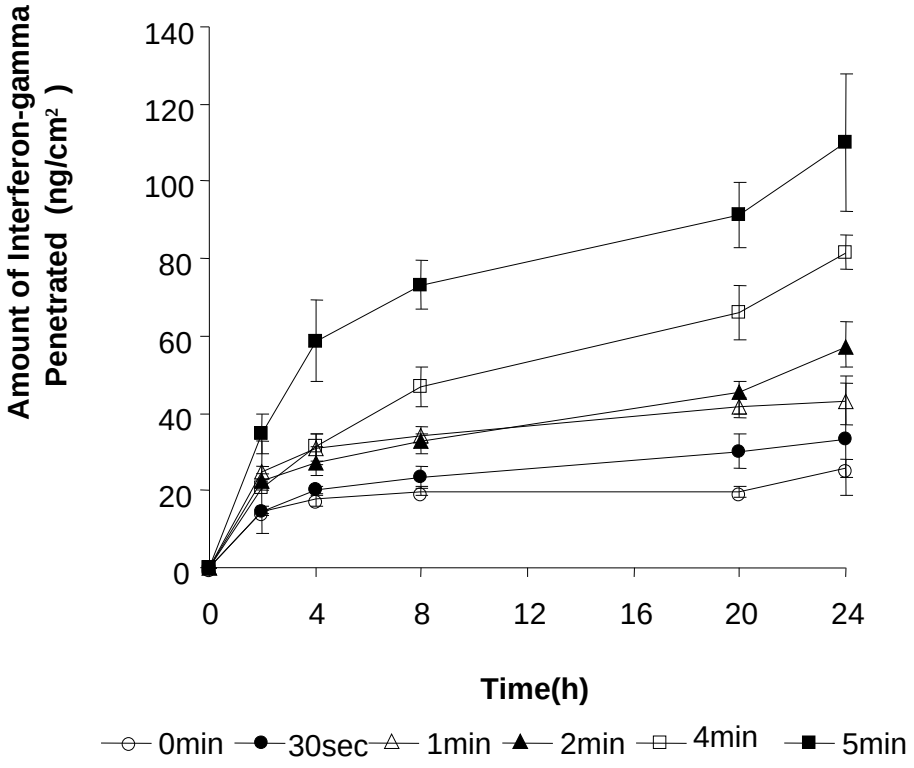

Fig. 3.6: Transdermal penetration profile of interferon-gamma following sodium lauryl sulphate pretreatment. Legend symbols refer to different sonication periods. Error bars indicate S.D. values, n=4.

Fig. 3.7 presents the permeation graphs relating to experiments involving SES pretreatment. It can be seen that without ultrasound, macromolecule flux was quite

high at the start so that the mean amount permeated was approximately 12 ng /cm^2 at 2 hours. However, from 2 hours onwards, the rate of drug flux through the skin was much lower but remained in a linear phase. By 24 hours, the mean amount permeated was about 20 ng /cm^2. As before, ultrasound application was observed to increase the initial burst of macromolecule transport. However, the correlation between ultrasound duration and magnitude of initial flux enhancement was unclear as many standard deviation values were quite large.

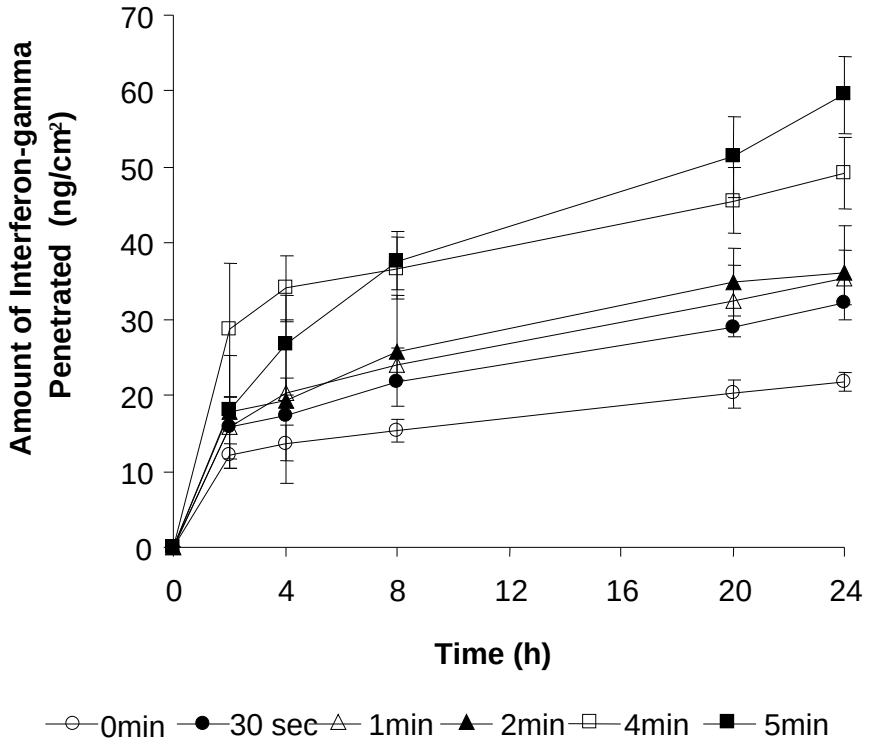

Fig. 3.7: Transdermal penetration profile of interferon-gamma following sodium eicosyl sulphate pretreatment. Legend symbols refer to different sonication periods. Error bars indicate S.D. values, n=4.

The duration of ultrasonication did not seem to greatly affect drug flux after 2 hours. Drug flux in this period was period was always lower than that in the first 2 hours

and was more or less constant, irrespective of sonication time. The exception to this was the longest 5 minute application, in which the rate was higher over 2 to 24 hours than in the other treatments.

It is normal to compare different treatments by plotting the linear or steady-state drug flux values. However, in these experiments the profiles were untypical and there were no single obvious steady state phases to plot. Hence, a comparison was made by plotting the amount of interferon-gamma permeated per unit area at 24 hours and this graph is shown in Fig. 3.8.

With regards to sonophoresis without chemical enhancers, it can be seen that macromolecule delivery increases with longer ultrasound application times. However, since the plot is somewhat erratic this means that the amount permeated does not increase in proportion to the application time. It can be seen that 2 minutes of ultrasound was almost as effective as 4 minutes and 5 minutes for enhancing interferon-gamma delivery.

With regards to ultrasound with either SOS or SES, it can be seen that these were more effective than ultrasound only at short ultrasound durations of 30s and 60s. However, at longer ultrasound durations these combined treatments were not more effective than ultrasound only.

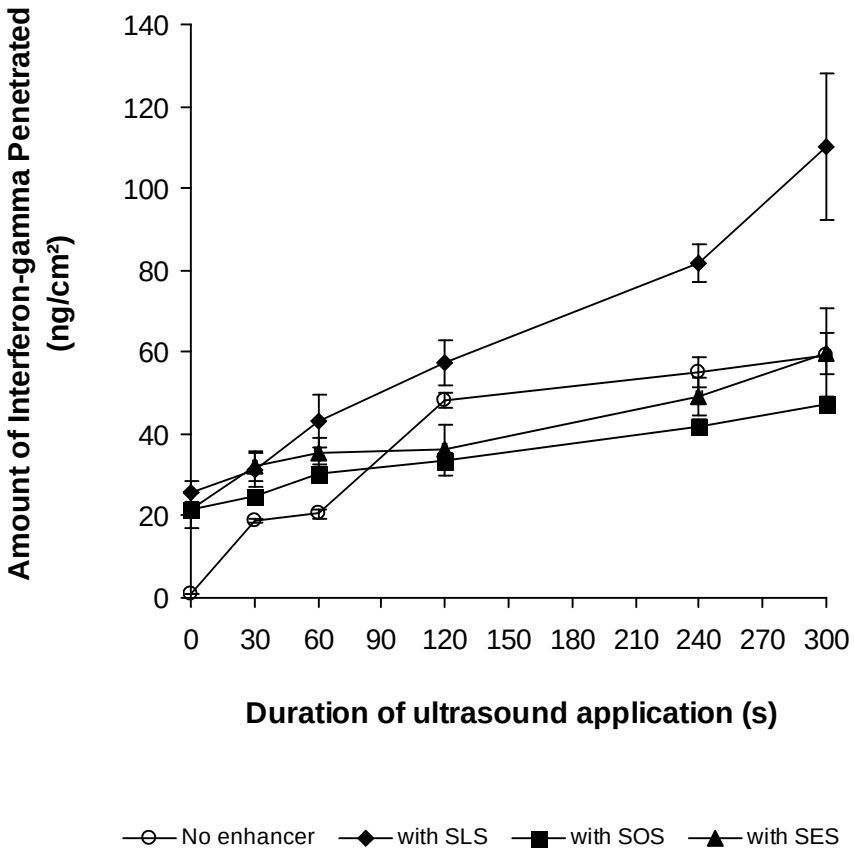

Fig. 3.8: Amount of interferon-gamma penetrated at 24 hours as a function of ultrasonication time. Legend symbols refer to different surfactant pretreatments. Error bars indicate S.D. values, n=4.

Of particular interest was the ultrasound with SLS combination treatment. Irrespective of sonication time, this combination was consistently and significantly more effective than ultrasound alone at permeabilising the skin to the macromolecule. In fact, 5 minutes sonophoresis with SLS pretreatment had the effect of almost doubling mean interferon-gamma cumulative permeation in comparison to sonophoresis alone.

3.3.3 Effects of Ultrasound and Terpenes

Fig. 3.9 shows the influence of 5 minutes of ultrasound application and / or menthone on interferon-gamma penetration through pig skin. It is clear that both menthone pretreatment only and menthone pretreatment followed by ultrasound were less effective than ultrasound alone in permeabilising the skin.

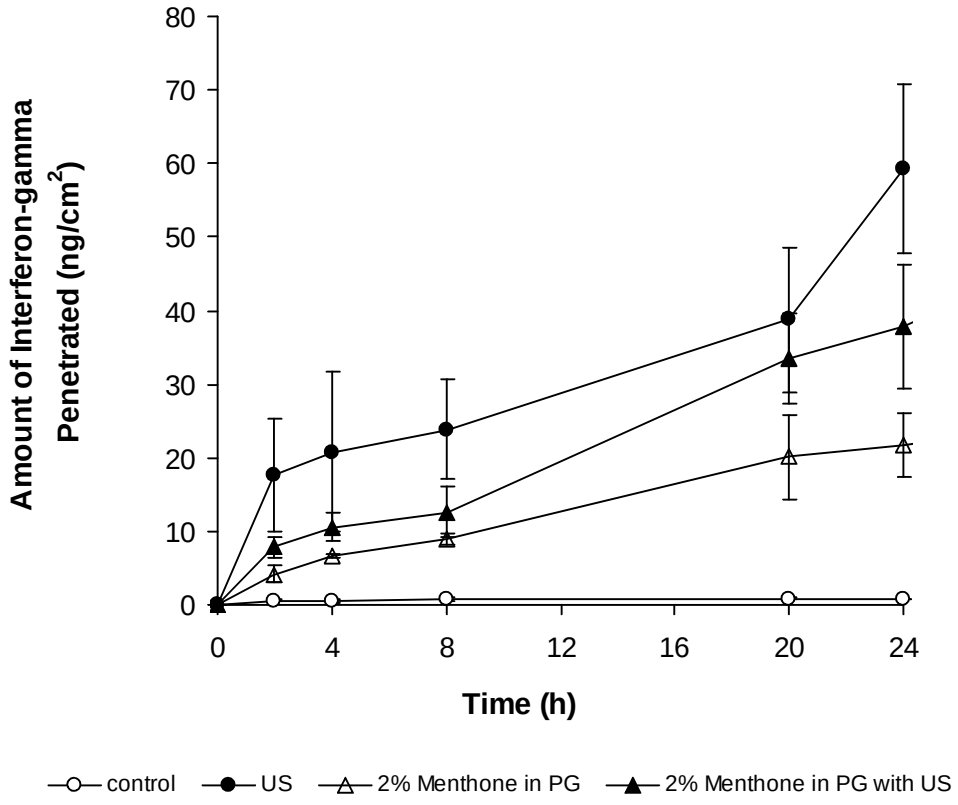

Fig. 3.9: Transdermal penetration profile of interferon-gamma following menthone pretreatment. Error bars indicate S.D. values, n=4.

Fig. 3.10 shows the permeation profiled obtained from the carvone studies. It can be seen that carvone pretreatment of skin, both with and without 5 minutes of

ultrasonication, acted to reduce drug penetration enhancement relative to ultrasonication alone.

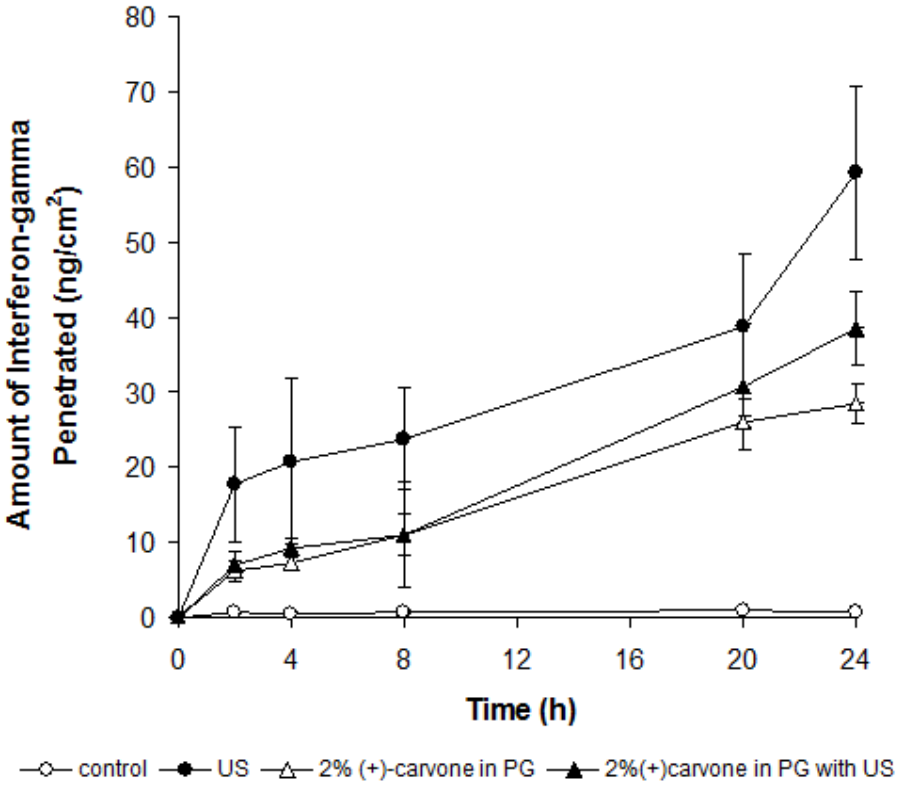

Fig. 3.10: Transdermal penetration profile of interferon-gamma following carvone pretreatment. Error bars indicate S.D. values, n=4.

Fig. 3.11 shows the effects of 5 minutes of ultrasound application and / or alpha terpineol pretreatment on cytokine flux through skin. It can be seen that alpha terpineol only produced less overall drug permeation than ultrasound exposure alone. The combination treatment was about as effective as ultrasound exposure alone.

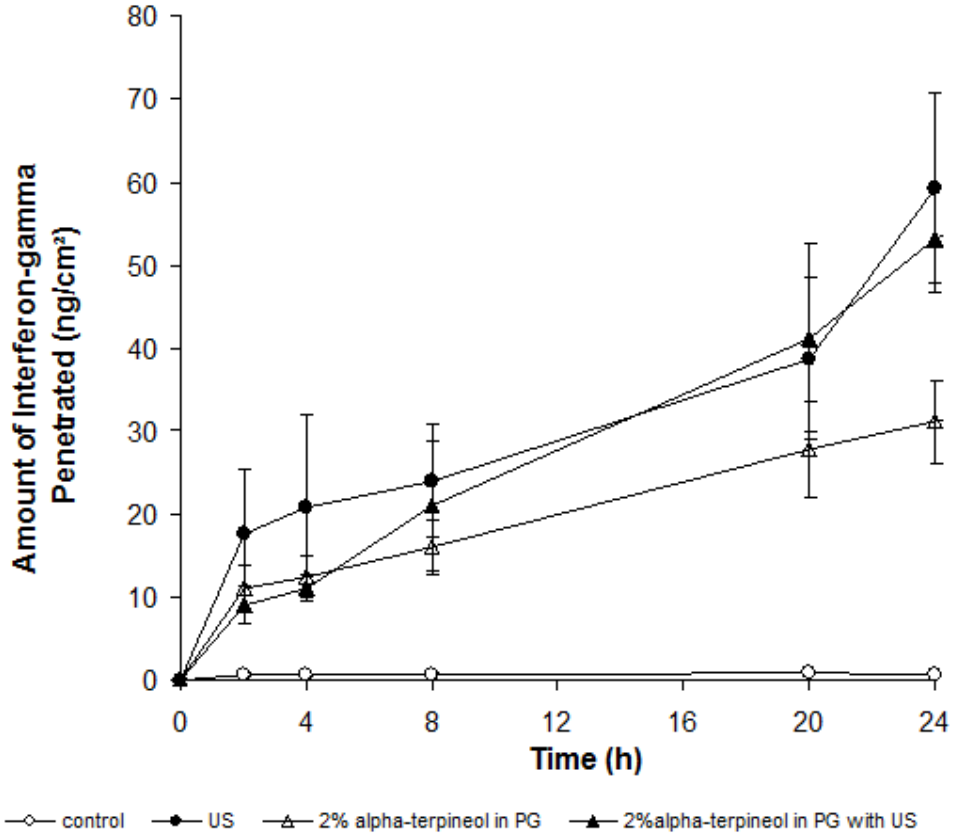

Fig. 3.11: Transdermal penetration profile of interferon-gamma following alpha-terpineol pretreatment. Error bars indicate S.D. values, n=4.

3.3.4 Effects of Ultrasound and Fatty Acids

Fig. 3.12 shows a plot of cumulative macromolecule permeation as a function of time for experiments involving stearic acid. It is apparent that 5 minutes of ultrasound alone was more effective at enhancing drug permeation than the two stearic acid treatments. In fact, skin treatment with stearic acid only produced an almost identical cumulative drug permeation profile to that of stearic acid followed by ultrasonication. This means that the presence of stearic acid some how eliminates the ultrasound effect on the stratum corneum.

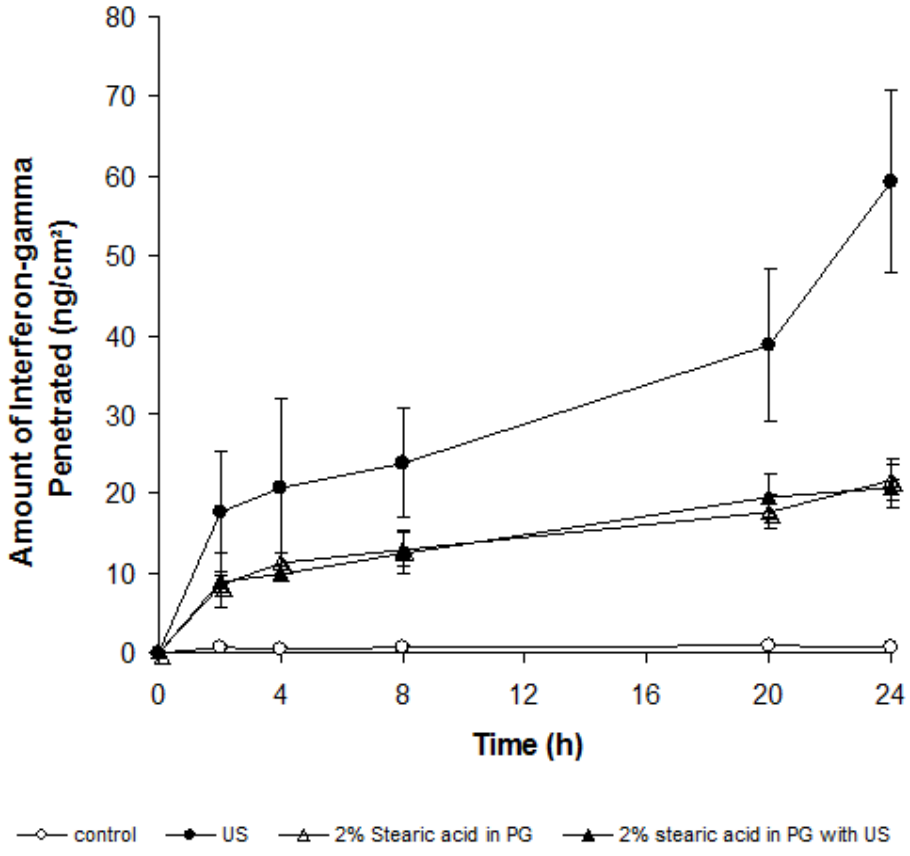

Fig. 3.12: Transdermal penetration profile of interferon-gamma following stearic acid pretreatment. Error bars indicate S.D. values, n=4.

The graph in Fig. 3.13 shows the influence of oleic acid and ultrasound on drug transport. It can be observed that oleic acid alone and oleic acid followed by sonication produced very similar cumulative drug permeation profiles. Both these treatments were significantly less enhancing than ultrasound only. Again, this suggests that the presence of this fatty acid somehow counteracts any ultrasound-induced changes in skin.

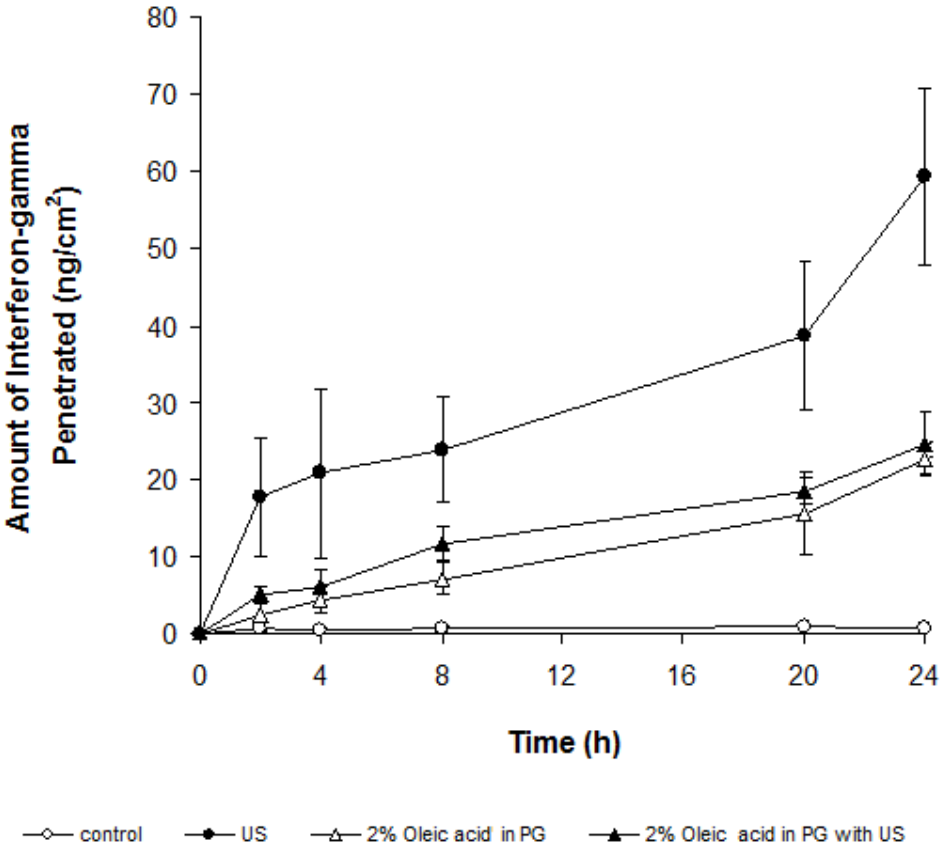

Fig. 3.13: Transdermal penetration profile of interferon-gamma following oleic acid pretreatment. Error bars indicate S.D. values, n=4.

Fig. 3.14 depicts the permeation profiles for the linoleic acid experiments. Again, chemical enhancer only and chemical enhancer followed by sonication produced quite similar macromolecule permeation profiles. Both these treatments were less effective at skin permeabilisation than ultrasound alone.

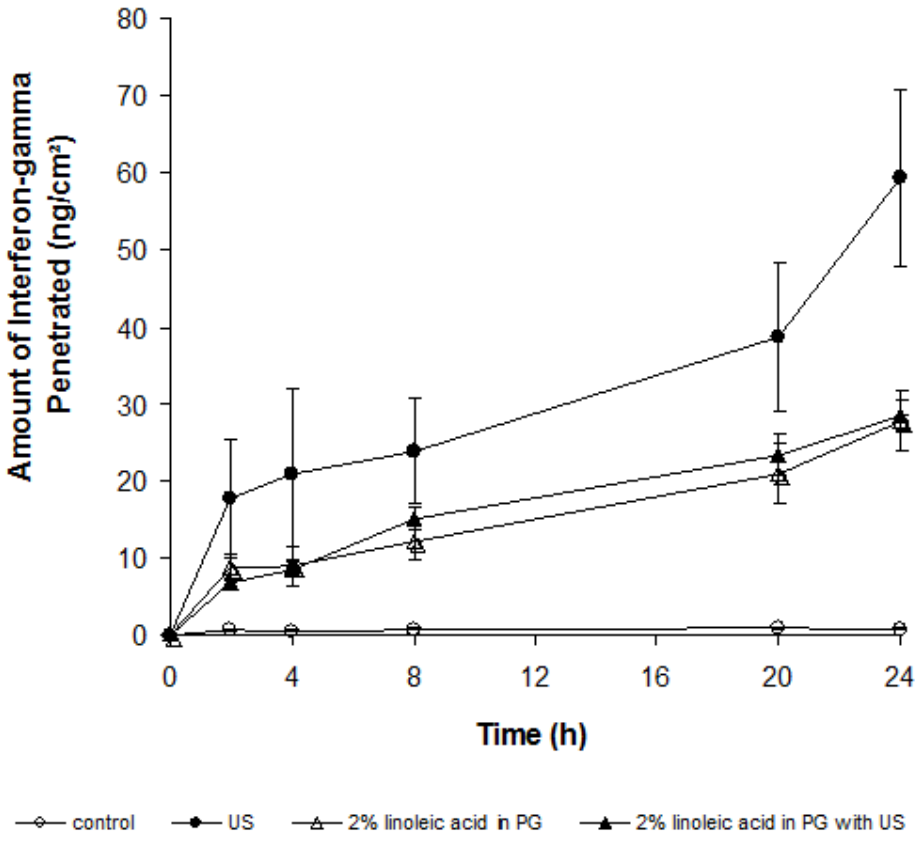

Fig. 3.14: Transdermal penetration profile of interferon-gamma following linoleic acid pretreatment. Error bars indicate S.D. values, n=4.

3.4. DISCUSSION

A general feature of these macromolecule transport studies was that while virtually no drug could passively permeate across full-thickness skin, the amounts permeating following 5 minutes of sonication were still very small. With sodium lauryl sulphate pretreatment, which proved to be the most effective combination, sonophoresis resulted in a mean cumulative permeation of about 110ng / cm^2 by 24 hours. This is a cytokine mass of approximately 70 ng or less than 0.002% of the total 4 x 10^6 ng available in the donor solution at time zero. Importantly, this mass of interferon-gamma in the receiver solution was structurally intact. This is due to the extremely high specificity of the ELISA assay used (Personal correspondence: Dr Dino Rotondo of Strathclyde University to S. Mohamed).

One important aspect was that the permeation profiles did not follow the usual lag time followed by linear steady state stage that is normally obtained in transdermal drug transport studies. As already proposed, this may be due to stratum corneum defects caused by ultrasound or chemical enhancers contracting after their removal. The defects become too small to allow macromolecule passage. Although this effect is not covered much in the literature reports, it has been discussed at scientific meetings (Personal Correspondence: Prof Richard Guy [University of Bath, UK] to Dr Victor Meidan [University of Strathclyde]).

An important result was that skin application of SLS followed by 20kHz ultrasound exposure caused an additive enhancement effect. In contrast, skin treatment with any of the other tested enhancers followed by ultrasound did not produce any additive

action. This confirms the findings of other groups who also found that SLS was very effective when combined with low frequency ultrasound (Mitragotri et al. 2000b; Tezel et al., 2002c; Lavon et al., 2005). Some of those studies reported much greater synergistic effects between ultrasound and SLS. It could be that the combination treatment is less effective when macromolecules are used rather than small molecular weight drugs.

CHAPTER 4: GENERAL CONCLUSIONS AND PROPOSALS FOR FURTHER RESEARCH

4.1 CONCLUSIONS

The first part of the experimental work (Chapter 2) aimed to validate the ultrasound output of the VCX-500 generator and transducer that were to be used in the later drug permeation studies. Hydrophone measurements showed that the actual frequency was very close (-0.6%) to the 20kHz value stated by the supplier. For intensity, the supplier's suggested method was checked against the 'in house-developed' calorimetric method. The calorimetrically-measured intensities were somewhat lower (~25%) than that measured by the manufacturer's method. Nevertheless, ultrasound output was consistent over time and the response varied in proportion to the amplitude dial setting on the generator. In conclusion, the VCX-500 generator and transducer were suitable for using as an ultrasound source in the current project.

The research described in Chapter 3 aimed to explore the use of 20kHz ultrasound and / or chemical enhancers for delivering the model macromolecule (interferon-gamma) transdermally. An in vitro Franz diffusion cell system was used with full-thickness pig skins employed as barrier. Pulsed ultrasound was applied under conditions that caused only very slight skin surface heating. Whereas passive macromolecule permeation was virtually zero, 5 minutes of ultrasound exposure

allowed about 50 ng /cm^2 of cytokine to permeate transdermally. Briefer ultrasound applications caused less drug permeation but the duration-cumulative permeation profile was not linear. Macromolecule delivery could be significantly improved by pretreating the skin with SLS before applying 5 minutes of ultrasound. This allowed macromolecule permeation to reach over 100 ng /cm^2. However, all other tested chemical enhancers – SOS, SES, menthone, carvone, alpha terpineol, oleic acid, linoleic acid and stearic acid did not show such an additive effect with ultrasound. The fact that only SLS showed a positive interaction with ultrasound fits in with the published literature that tends to focus overwhelmingly on SLS sonophoresis.

4.2 IDEAS FOR FURTHER INVESTIGATION

Many of the literature reports describe much greater SLS - low frequency transport enhancements than the values determined in the current study. This may be because those previous studies used epidermal membranes or split-thickness skins rather than the full-thickness samples used in this project. Such thinner membranes might be more susceptible to ultrasound-induced changes, partially because those membranes absorb more of the acoustic energy than thicker tissues. Hence, further work could involve repeating some of the studies performed in this project but using epidermal or dermatomed skins while keeping all other variables unchanged. It may be possible to determine how low frequency ultrasound interacts with different skin strata. Another option for further research would be to repeat the key studies using human skin, which is of course the most relevant model. Again, use of heat-separated human epidermal membranes or isolated dermal tissue might give clues

about mechanisms. Changing the order and / or time period between sonication and drug application may also provide more information.

Further work could also focus on the ultrasound itself. Other published studies describe use of a transducer that is wider than the 3mm diameter one used here and that emits a greater acoustic power. So another option would be to repeat some of the studies described in this project but using a wider transducer. Use of a different generator type that emits a different ultrasound frequency may also be of interest.

An important finding of the current project was that interferon-gamma permeation did not follow the classic lag time followed by linear steady state phase that is typical of transdermal drug permeation. Although a mechanism for this has been proposed, it would be interesting to repeat the current study but using a completely different macromolecule, perhaps also utilising a different assay method. Such an approach may show whether non-typical transdermal permeation profiles occur for other macromolecules. The possibility of precipitation could be investigated by conducting optical turbidity measurements of the donor solution after sonication.

It would be interesting to run the SLS-sonophoresis experiments but using another macromolecule that has an actual clinical use like low molecular weight heparin or insulin. This would allow a measure of whether the technique is delivering anywhere near the therapeutic target range within the systemic circulation.

Finally, very little is known of the possible harmful influences of low frequency ultrasound. So exposing various skin tissues or even isolated kerotinocytes in solution to ultrasound and running tests for viability, apoptosis or oxidation would be useful. Such tests could be performed before exploring the effects of low frequency ultrasound in human clinical studies.

REFERENCES

Alvarez-Román, R., Merino, G., Kalia, Y.N., Naik, A., Guy, R.H. 2003. Skin Permeability Enhancement by Low Frequency Sonophoresis: Lipid Extraction and Transport Pathways. J. Pharm. Sci. 92, 1138–1146.

Asbill, C.S., Michniak, B.B. 2000. Percutaneous penetration enhancers: local versus transdermal activity. Pharm. Sci. Technol. Today 3, 36-41.

Barry, B.W. 1983. Dermatological formulations percutaneous absorption. In: Barry, B.W. (Eds.). Marcel Dekker, New York.

Barry, B.W. 2001. Is transdermal research still important today? Drug Discovery Today. 6, 967- 971.

Blank, H.I., Scheuplein, R.J., 1969. Transport into and within the skin. Br. J. Dermatol. 81, 4-10.

Boucaud, A., Machet, L., Arbeille, B., Machet, M.C., Sournac, M., Mavon, A., Patat, F., Vaillant, L., 2001a. *In vitro* study of low-frequency ultrasound-enhanced transdermal transport of fentanyl and caffeine across human and hairless rat skin, Int. J. Pharm. 228, 69−77.

Boucaud, A., Garrigue, M.A., Machet, L., Vaillant, L., Patat, F. 2002. Effect of sonication parameters on transdermal delivery of insulin to hairless rats. J. Control. Rel. 81, 113−119.

Bucks, D., Maibach, H.I. 1999. Occlusion does not uniformly enhance penetration in vivo. In: Topical Absorption of Dermatological Products, Bronaugh, R.L., Maibach, H.I. (Eds.) Informa Health Care, New York. pp 9-32.

Borrás-Blasco J, Díez-Sales O, López A, Herráez-Domínguez M. 2004. A mathematical approach to predicting the percutaneous absorption enhancing effect of sodium lauryl sulphate. Int. J. Pharm. 269, 121-129.

Cantrell, J.T., McArthur, M.J., Pihko, M.V. 2000. Transdermal extraction of interstitial fluid by low frequency ultrasound quantified with $^{3}H_2O$ as a tracer molecule. J. Pharm. Sci. 89, 1170-1179.

Chivers, R.C. 1991. Fundamentals of ultrasonic propagation. In: Output Measurements for Medical Ultrasound, Preston R. (Ed.) Springer, London. pp 19-33.

Doukas, A.G., Kollias, N. 2004. Transdermal drug delivery with a pressure wave. Adv. Drug Deliv. Rev. 56, 559-579.

El-Kattan, A.F., Asbill, C.S., Kim, N., Michniak, B.B. 2001. The effects of terpene enhancers on the percutaneous permeation of drugs with different lipophilicities. Int. J. Pharm. 215, 229-240.

Elyan, B.M., Sidhom, M.B., Plakogiannis, F.M. 1996. Evaluation of the effect of different fatty acids on the percutaneous absorption of metaproterenol sulfate. J. Pharm. Sci. 85, 101-105.

Fang, J.-You, Fang, C.-Lang, Sung, K.C., Chen, H.-Yin, 1999. Effect of low frequency ultrasound on the *in vitro* percutaneous absorption of clobetasol 17-propionate, Int. J. Pharm. 191, 33−42.

Frum, Y., Eccleston, G.M., Meidan, V.M., 2008. In vitro permeation of drugs into porcine hair follicles. Is it quantitatively equivalent to permeation into human hair follicles? J. Pharm. Pharmacol. 60, 434-439.

Frum Y., Khan, G.M., Sefcik, J., Rouse, J., Eccleston, G.M., Meidan, V.M., 2007. Towards a correlation between drug properties and in vitro transdermal flux variability. Int. J. Pharm. 336, 140-147.

Godin, B. Touitou, E. 2007. Transdermal skin delivery: predictions for humans from in vivo, ex vivo and animal models. Adv. Drug Delivf. Revs. 59, 1152-1161.

Godwin, D.A., Michniak, B.B. 1999. Influence of drug lipophilicity on terpenes as transdermal penetration enhancers. Drug Devel. Ind. Pharm. 25, 905-915.

Hadgraft J., 2004. Skin deep. Eur. J. Pharm. Biopharm. 58, 291-299.

Hastie, C. 2008. Interferon-gamma. A possible therapeutic option for late stage prostate cancer. Anticancer Res. 28, 2843-2849.

Khan, G.M., Frum, Y., Sarheed, O., Eccleston, G.M., Meidan, V.M. 2005. Assessment of drug permeability distributions in two different model skins. Int. J. Pharm. 303, 81-87.

Katz, N.P., Shapiro, D.E., Hermann, T.E., Kost, J., Custer, L.M. 2004. Rapid onset of cutaneous anesthesia with EMLA cream after pretretament with a new ultrasound-emitting device. Anes. Anal. 98, 371-376.

Kimura, T., Sakamoto, T., Leveque, J., Sohmiya, H., Fujita, M., Ikeda, S., Ando, T. 1996. Standardization of ultrasonic power for sonochemical reaction. Ultrason. Sonochem. 3, S157-S161.

Knorr, F., Lademann, J., Patzelt, A., Sterry, W., Blume-Peytavi, U., Vogt, A. 2009. Follicular transport route--research progress and future perspectives. Eur. J. Pharm. Biopharm. 71, 173-180.

Kost, J., Mitragotri S., Gabbay, R.A., Pishko, M., Langer, R. 2000. Transdermal monitoring of glucose and other analytes using ultrasound. Nat. Med. 6, 347-350.

Kushner, J., Blankschtein, D., Langer, R., 2008. Evaluation of hydrophilic permeant transport parameters in the localized and non-localized transport regiosn of skin treated simultaneousl with low frequency ultrasound and sodium lauryl sulphate. J. Pharm. Sci. 97, 906-918.

Lavon, I., Grossman, N., Kost, J., 2005. The nature of ultrasound-SLS synergism during enhanced transdermal transport. J. .Control. Release 107, 484-94.

Lavon, I., Grossman, N., Kost, J., Kimmel, E., Ended, G., (2007). Bubble growth within the skin might play a significant role in sonophoresis. J. control. Rel. 117, 246-255.

Leveque, N., Raghavan, S.L., Lane, M.E., Hadgraft, J., 2006. Use of a molecular form technique for the penetration of supersaturated solutions of salicylic acid across silicone membranes and human skin in vitro. Int. J. Pharm. 318, 49-54.

Meidan, V.M., Bonner, M.C., Michniak, B.B. 2005. Transfollicular drug delivery – is it a reality? Int. J. Pharm. 306, 1-14.

Meidan, V.M., Michniak, B.B. 2004. Emerging technologies in transdermal therapeutics. Am. J. Ther. 11, 312-316.

Meidan, V.M., Roper, C.S., 2008. Inter and intra-individual variability in human skin barrier function: A large scale retrospective study. Toxicol. In Vitro. 22, 1062-1069.

Merino, G., Kalia, Y.N., Delgado-Charro, M.B., Potts, R.O., Guy, R.H. 2003. Frequency and thermal effects on the enhancement of transdermal transport by sonophoresis. J. Control. Release. 88, 85–94.

Merisko-Liversidge, E.M., Liversidge, G.G. 2008. Drug nanoparticles: formulating poorly water-soluble compounds. Toxicol. Pathol. 36, 43-48.

Mitragotri, S. 2003. Modeling skin permeability to hydrophilic and hydrophobic solutes based on four permeation pathways. J. Control. Release 86, 69-92.

Mitragotri S., Blankschtein D, Langer R. 1995a. Ultrasound-mediated transdermal protein delivery. Science 269, 850−853.

Mitragotri S., Blankschtein D, Langer R. 1996. Transdermal delivery using low frequency sonophoresis. Pharm. Res. 13, 411-420.

Mitragotri, S., Kost, J. 2000. Low frequency sonophoresis: a noninvasive method of drug delivery and diagnostics. Biotechnol. Prog. 16, 488-492.

Mitragotri, S., Kost, J. 2001. Transdermal delivery of heparin and low- molecular weight heparin using low frequency ultrasound. Pharm. Res. 18, 1151−1156.

Mitragotri, S., Edwards, D.A., Blankschtein, D., Langer, R. 1995b. A mechanistic study of ultrasonically-enhanced transdermal drug delivery. J. Pharm. Sci. 84, 697−706.

Mittal, A., Sara, U.V., Ali A., Aqil, M. 2009. Status of fatty acids as skin penetration enhancers – a review. Current Drug Deliv. 6, 274-279.

Monti, D., Giannelli, R., Chetoni, P., Burgalassi, S. 2001. Comparison of the effect of ultrasound and of chemical enhancers on transdermal permeation of caffeine and morphine through hairless mouse skin in vitro. Int. J. Pharm. 229, 131−137.

Mutoh, M., Ueda, H., Nakamura, Y., Hirayama, K., Atobe, M., Kobayashi, D., Morimoto, Y. 2003. Characterization of transdermal solute transport induced by low-frequency ultrasound in the hairless rat skin. J. Control. Release 92, 137−146.

Okabe H., Obata, Y., Takayama, K., Nagai, T., 1990, Percutaneous absorption enhancing effect and skin irritation of monocyclic monoterpenes. Drug Des. Deliv. 6, 229-238.

Paliwal, S., Menon, G.K., Mitragotri, S. 2006. Low-frequency sonophoresis: ultrastructural basis for stratum corneum permeability assessed using quantum dots. J. Invest. Dermatol. 126, 1095-1101.

Park E.J., Werner J., Smith N.B. 2007. Ultrasound mediated transdermal insulin delivery in pigs using a lightweight transducer. Pharm Res. 24, 1396-1401.

Preston, R. 1991. In: Output Measurements for Medical Ultrasound, Springer, London.

Rao, R.., Nanda, S. 2009. Sonophoresis: recent advancements and future trends. J. Pharm. Pharmacol. 61, 689-705.

Riviere, J.E. 1993. Biological factors in absorption and permeation. In: Zatu JL (Ed.). Skin Permeation. Fundamentals and Application. Wheaton, Allured, pp113-126.

Rowat, A.C., Kitson, N., Thewalt, J.L. 2006. Interactions of oleic acid and model stratum corneum membranes as seen by ^{2}H-NMR. Int. J. Pharm. 307, 225-231.

Santoainni, P., Nino, M., Calabro, G. 2004. Intradermal drug delivery by low frequency sonophoresis (25 kHz). Dermatol. Online J. 10, 24.

Schaefer, H., Redelmeier, T.E. 1996. Skin barrier principles of percutaneous absorption. In: Schaefer, H., Redelmeier, T.E. (Eds.). Karger, Basel.

Scheuplein , R.J., Blank, I.H., 1971. Permeability of the skin. Physiol. Rev. 51, 701-747.

Sznitowska, M., Janicki, S., Baczek, A., 2001. Studies on the effect of pH on the lipoidal route of penetration across the stratum corneum. J. Control. Release 76, 327-335.

Tachibana, K., 1992. Transdermal delivery of insulin to Alloxan-Diabetic Rabbits by Ultrasound Exposure. Pharm. Res. 9, 952−954.

Tachibana, K., Tachibana, S., 1991. Transdermal delivery of ultrasonic vibration. J. Pharm. Pharmacol. 43, 270−271.

Tachibana, K., Tachibana, S., 1993. Use of ultrasound to enhance the local anaesthetic effect of topically applied aqueous lidocaine. Anaesthesiology 78, 1091−1096.

Teo, K.C., Xu, Y., Yang, C., 2001. Sonochemical degradation for toxic halogenated organic compounds. Ultrason. Sonochem. 8, 241-246.

Terahara, T., Mitragotri, S., Langer, R. 2002. Porous resins as a cavitation enhancer for low frequency sonophoresis. J. Pharm. Sci. 91, 753-759.

Tezel A, Sens A, Tuchscherer J, Mitragotri S. 2002c. Synergistic effect of low-frequency ultrasound and surfactants on skin permeability. J. Pharm. Sci. 91, 91-100.

Tezel, A., Mitragotri, S. 2003. Interactions of inertial cavitation bubbles with stratum corneum lipid bilayers during low-frequency sonophoresis. Biophysical J. 85, 3502–3512.

Tezel, A., Paliwal, S., Shen, Z., Mitragotri, S. 2005. Low frequency ultrasound as a transcutaneous immunization agent. Vaccine. 23, 3800-3807.

Tezel A., Sens A., and Mitragotri S. 2002a Incorporation of lipophilic pathways into the porous pathway model for describing skin permeabilization during low frequency sonophoresis. J. Control. Rel. 83: 183-188.

Tezel, A., Sens, A., Mitragotri, S., 2002b. Investigations of the role of cavitation in low-frequency sonophoresis using acoustic spectroscopy. J. Pharm. Sci. 91, 444−453.

Uitto, J. 1993. Biology of dermatological cells and extracellular matrix. In: Fitzpatrick, T.B., Eisen, A.Z., Wolff, K., Freedberg, I.M., Austen KF (Eds.). Dermatology in General Medicine. McGraw-Hill, pp221-240.

Vaddi, H.K., Ho, P.C., Chan, S.Y. 2002. Terpenes in propylene glycol as skin-penetration enhancers: permeation and partition of haloperidol, Fourier transform infrared spectroscopy, and differential scanning calorimetry. J. Pharm. Sci. 91, 1639-1651.

Verdier-Sévrain S, Bonté F., 2007. Skin hydration: a review on its molecular mechanisms. J. Cosmet. Dermatol. 6, 75-82.

Walker, W., Rotondo, D. 2004. Prostaglandin E2 is a potent regulator of interleukin-12- and interleukin-18-induced natural killer cell interferon-gamma synthesis. Immunology 111, 298-305.

Williams, A.C., Barry B.W., 2004. Penetration enhancers. Adv. Drug Deliv. Revs. 56, 603-618.

Williams, A.R. (1983) Ultrasound: Biological effects and potential hazards. Academic Press, London.

Wilhelm, K.P., Surber, C., Maibach, H.I. 1991. Effect of sodium lauryl sulfate-induced skin irritation on in vivo percutaneous penetration of four drugs. J. Invest. Dermatol. 97, 927-932.

Wu, J., Chappelow, J., Yang, J., Weimann, L. 1998. Defects generated in human stratum corneum specimens by ultrasound. Ultrasound Med. Biol. 24, 705−710.

Yamashita N., Tachibana K., Ogawa K., Tsujita N., and Tomita A. 1997. Scanning electron microscopic evaluation of the skin surface after ultrasound exposure. Anat. Rec. 247: 455-461.

Yuan, Y, Verma R. 2006. Measuring microelastic properties of stratum corneum. Coll. Surf. B: Biointerfaces 48, 6-12.